Fire resistance prediction of slim-floor asymmetric steel beams using single hidden layer ANN models that employ multiple activation functions

Panagiotis G. Asteris[1], Chrysanthos Maraveas[2], Athanasios T. Chountalas[1], Dimitrios S. Sophianopoulos[3] and Naveed Alam[4]

[1]*Computational Mechanics Laboratory, School of Pedagogical and Technological Education, 14121 Athens, Greece*
[2] *Department of Natural Resources and Agricultural Engineering, Agricultural University of Athens, Greece*
[3]*Department of Civil Engineering, University of Thessaly, Volos, Greece*
[4] *FireSERT, School of Built Environment, Ulster University, Belfast, UK*

(Received keep as blank , Revised keep as blank , Accepted keep as blank)

Abstract. In this paper a mathematical model for the prediction of the fire resistance of slim-floor steel beams based on an Artificial Neural Network modeling procedure is presented. The artificial neural network models are trained and tested using an analytical database compiled for this purpose from analytical results based on FEM. The proposed model was selected as the optimum from a plethora of alternatives, employing different activation functions in the context of Artificial Neural Network technique. The performance of the developed model was compared against analytical results, employing several performance indices. It was found that the proposed model achieves remarkably improved predictions of the fire resistance of slim-floor steel beams. Moreover, based on the optimum developed AN model a closed-form equation for the estimation of fire resistance is derived, which can prove a useful tool for researchers and engineers, while at the same time can effectively support the teaching of this subject at an academic level.

Keywords: Activation Functions; Artificial Neural Networks; Slim-floor steel beams; Fire resistance; Soft Computing

Nomenclature

a10-index	Performance index
ANN(s)	Artificial Neural Network(s)
[bi]	Bias matrix of the hidden layer
[bo]	Bias matrix of the output layer
BPNN	Back Propagation Neural Network
CCC	Concrete compressive Strength
CFST	Concrete Filled Steel Tube
d	Depth of structural element
E_d	The design value of the corresponding force for a fundamental combination of actions
$E_{fi,d}$	Design forces for fire situation
f'_c	Concrete Compressive Strength
f_y	Steel Yield Limit
f_u	Steel Ultimate Strength
FR	Fire Resistance
GP	Genetic Programming
GUI	Graphical User Interface
HTS	Hyperbolic Tangent Sigmoid transfer function
[IP]	Matrix of the input parameters
[Iw]	Weight matrix of the hidden layer
L	Clear span of a simply supported beam
Li	Linear transfer function
LS	Log-Sigmoid transfer function
[L_W]	Weight matrix of the output layer
MAPE	Mean Absolute Percentage Error
MSE	Mean Square Error
n_{fi}	Load Factor
NRB	Normalized Radial Basis transfer function
PLi	Positive Linear transfer function
R	Pearson correlation coefficient
RB	Radial Basis transfer function
SL	Span Length
SM	Soft Max transfer function
SSE	Sum Square Error
SSL	Symmetric Saturating Linear transfer function
SYS	Steel Yield Strength
TB	Triangular Basis transfer function

1. Introduction

Steel-concrete composite structures have several benefits compared with conventional steel or reinforced concrete structures. Amongst the main advantages of composite construction, their enhanced fire performance is of high significance, owing to the heat sink effect provided by the concrete. This effect delays the temperature rise in composite sections as compared with bare steel solutions.

Steel-concrete composite flooring systems have been developed since 19th century in the form of jack arch floors (Ahmed and Tsavdaridis 2019, Maraveas *et al.* 2013), and new developments are presented up to today. These new developments include various types of slim floors including the Delta beams, Ultra Shallow Floor Beams, etc. (Ahmed and Tsavdaridis 2019).

The fire resistance of these flooring systems is complex, given that the unprotected bottom flange develops high temperatures when exposed to fire. The rest of the steel cross section is protected by concrete and develops low temperatures even in longer exposure to fire. Therefore, the temperature distribution within the height of these beams is extremely nonlinear (Bailey 1999, Maraveas *et al.* 2014, Maraveas *et al.* 2017a), and bowing effects are developed both along the length as well as across the cross-section.

Although research on the fire resistance of these flooring systems have been initiated many decades ago including these from the past (Bailey 1999, Walnman 1996, Ma and Mäkeläinen 2000, Bailey 2003, Mäkeläinen and Ma 2000, Ma and Mäkeläinen 2006) and the recent ones included in the references (Ellobody 2011, *Kim et al. 2011*, Ahn and Lee 2017, Albero *et al.* 2019, Albero *et al.* 2020, Alam *et al.* 2021a, Alam *et al.* 2021b). In addition, several developments on the fire resistance evaluation have also been published (Both *et al.* 1997, Romero *et al.* 2015, Romero *et al.* 2019, Romero *et al.* 2020, Zaharia and Franssen 2012). Despite all these efforts, the fire resistance evaluation procedure remains complex as reviewed by Memarzadeh *et al.* (2021).

As per EN1994-1-2, all methodologies propose a two-step procedure, first the temperatures are calculated (according analytical or numerical methods) and second the moment capacity of the composite beam is calculated for the reduced material properties considering the higher temperatures expected to be achieved in a fire scenario. If the moment capacity is not found to be higher than the fire design moment, the procedure should be repeated for another cross section. Most methods focus on the simplification of temperatures calculation and EN1994-1-2 proposed a method too. The accuracy of these methods is low (Alam *et al.* 2021b) and combination of these methods is needed to evaluate accurately the temperatures developed on different parts of these beams. Furthermore, practicing engineers are not familiar with temperatures and have difficulties to undertake these calculations.

The increasing interest in steel-concrete composite structures, such as slim-floor asymmetric steel beams in contemporary buildings, highlights the necessity for a more thorough understanding of this valuable type of composite structural material. Taking into account the multiple geometrical and mechanical parameters of slim-floor asymmetric steel-concrete beams, which affect their fire resistance in a highly non-linear manner, soft computing techniques emerge as the tool that can be implemented to shed light on this composite structural element. This can assist in the better understanding of the material, as well as in design optimization processes in an integrated space, something that has not been possible until now.

The use of soft computing techniques for the prediction of the mechanical characteristics has already been the subject of research for composite structures such as for the prediction of ultimate axial load of concrete-filled steel tube columns (Sarir *et al.* 2019, Le *et al.* 2021, Ly *et al.* 2021 and Asteris *et al.* 2021a), the compressive strength of concrete materials (Özcan *et al.* 2009, Bilim *et al.* 2009, Duan *et al.* 2013, Asteris and Mokos 2020, Duan *et al.* 2020, Asteris *et al.* 2021b, Asteris *et al*. 2021c and Asteris *et al*. 2021d) and for the prediction of cement mortar compressive strength (Apostolopoulou *et al.* 2019, Asteris *et al.* 2019, Apostolopoulou *et al.* 2020). The use of soft computing techniques has been highlighted in many studies in the field of civil engineering (Kechagias *et al.* 2018, Psyllaki *et al.* 2018, Huang *et al.* 2019, Zeng *et al.* 2021, Zhang *et al.* 2021).

In the light of the above, a plethora of artificial neural networks has been trained and developed using a big Finite Element Method-based analytical database and ten different activations functions. Among them, the optimum ANN model for the Fire resistance prediction of slim-floor asymmetric steel beams is that which achieved the best performance indices.

At this point, it is worth noting that the Artificial Neural networks models have been accused of acting as black boxes which, although they can predict a parameter of the problem under study for which they have been developed and trained, they do not allow the user to understand how it works and how the input parameters affect the value of the estimated parameter. In the present work, following previous recent work of the authors (Asteris *et al.* 2021a, Zeng *et al.* 2021, Le *et al.* 2021), based on the optimal artificial neural network, the authors extract and present a closed-form equation for the estimation of fire resistance based on the optimum ANN model. The derived equation can prove a useful tool for researchers and engineers, as it reveals the strong linear nature of the fire resistance of slim-floor asymmetric steel beams (Fig. 1) with the involved parameters, while at the same time can effectively support the teaching of this subject at an academic level.

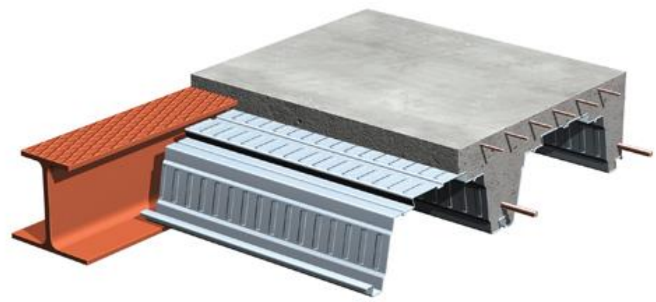

Fig. 1 Typical asymmetric slim floor beam layout

2. Materials and methods

2.1 Brief Review on Artificial Neural Networks

Artificial neural networks (ANNs) are based on the concept of the biological neural network of the human brain. The basic building block of ANNs is the artificial neuron, which is a mathematical model aiming to mimic the behavior of the biological neuron (Fig. 2).

Information is passed into the artificial neuron as input and is processed with a mathematical function leading to an output that determines the behavior of the neuron (similar to fire-or-not situation for the biological neuron). Before the information enters the neuron, it is weighted in order to approximate the random nature of the biological neuron. A group of such neurons consists of an ANN, in a manner similar to biological neural networks. In order to set up an ANN, one needs to define: (i) the architecture of the ANN; (ii) the training algorithm, which will be used for the ANN's learning phase; and (iii) the mathematical functions describing the mathematical model.

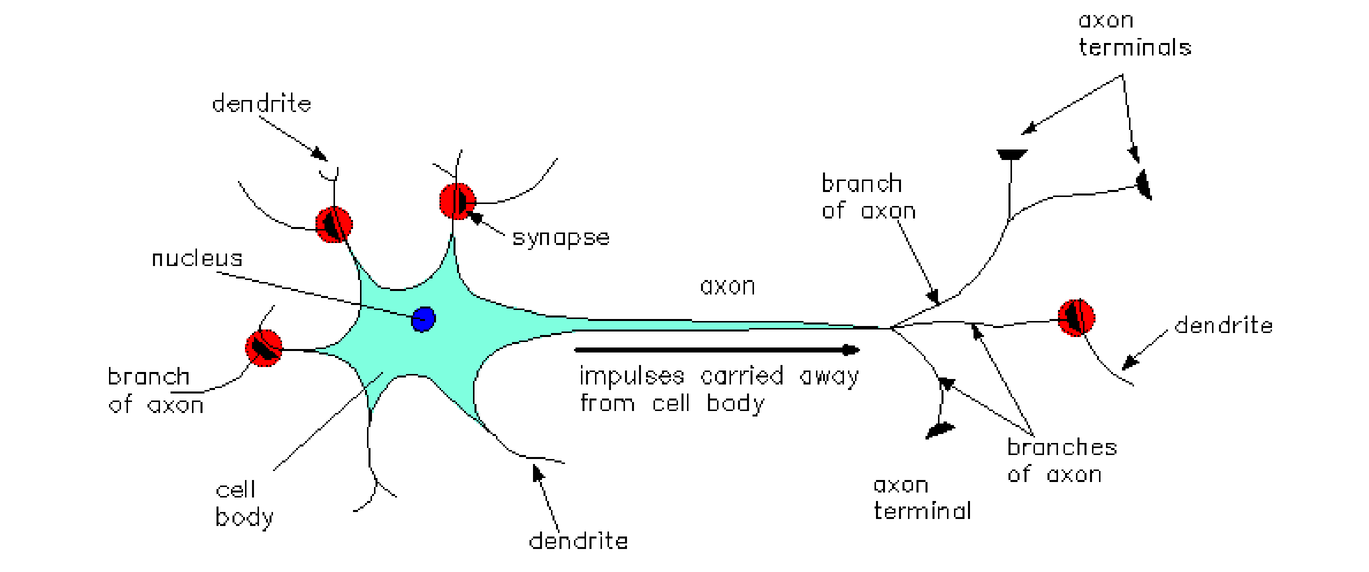

Fig. 2 Schematic representation of the biological neuron structure (Asteris et al. 2019)

The architecture or topology of the ANN describes the manner in which the artificial neurons are organized in the group and how information flows within the network. For example, if the neurons are organized in more than one layer, then the network is called a multilayer ANN. The training phase can be considered as a function minimization problem, in which the optimum values of weights need to be determined by minimizing an error function. Depending on the optimization algorithms used for this purpose, different types of ANNs exist. The gradient descent (GD) method is employed mainly in the back-propagation (BP) stage of the training process of the ANN model (Rumelhart *et al.* 1986). The main working principle of the GD is to adjust the weights of the ANN model iteratively while minimizing the error between the actual output and target (Du and Swamy 2013). However, using GD may results to convergence problems (Gupta *et al.* 2013) (i.e., time-consuming training process). Many more training algorithms have been proposed to enhance the effectiveness of ANN training, one of them is the Levenberg-Marquardt (LM) method (Marquardt 1963), which has been commonly used in various studies of different fields (Raghuwanshi *et al.* 2006, Aqil *et al.* 2007, de Vos and Rientjes 2008, Taormina *et al.* 2012). The speed of convergence when using the LM technique has been improved due to the method that was developed by combining the GD and Gauss-Newton (GN) algorithms (Marquardt 1963). More recently, a number of training algorithms that use the second derivative have been proposed in the literature. These are the One-Step Secant (OSS) (Battiti 1992), the Gradient Descent with Adaptive Learning Rate (GDA) (Kayacan and Khanesar 2015), the Scaled Conjugate Gradient (SCG) (Møller 1993), and the Conjugate Gradient Backpropagation with Powell-Beale Restarts (CGB) (Powell 1977). However, second-order learning techniques require to be used in a batch mode due to the sensitivity of the numerical computation of second-order gradients (Akbar *et al.* 2011, Du and Swamy 2013). In addition, learning algorithms based on the first and second-order derivative may not have the required convergence ability if the starting point is located outside of the search domain (Brownlee 2016). The foresaid learning algorithms contributed to the progress in training ANN methods, for better performance of the prediction models.

2.2 Performance Indices

Three different statistical parameters were employed to evaluate the performance of the derived computational model as well as the available in the literature formulae, including the root mean square error (RMSE), the mean absolute percentage error (MAPE), and the Pearson Correlation Coefficient R^2. The lower RMSE and MAPE values represent the more accurate prediction results. The higher R^2 values represent the greater fit between the analytical and predicted values. The aforementioned statistical parameters have been calculated by the following expressions (Alavi and Gandomi 2012):

$RMSE = \sqrt{\frac{1}{n}\sum_{i=1}^{n}(x_i - y_i)^2}$	(1)
$MAPE = \frac{1}{n}\sum_{i=1}^{n}\left\lvert\frac{x_i - y_i}{x_i}\right\rvert$	(2)
$R^2 = 1 - \left(\frac{\sum_{i=1}^{n}(x_i - y_i)^2}{\sum_{i=1}^{n}(x_i - \bar{x})^2}\right)$	(3)

where n denotes the total number of datasets, and x_i and y_i represent the predicted and target values, respectively.

The reliability and accuracy of the developed neural networks were evaluated using Pearson's correlation coefficient R and the root mean square error (RMSE). RMSE presents information on the short-term efficiency which is a benchmark of the difference of predicted values in relation to the experimental values. The lower the RMSE, the more accurate is the evaluation. The Pearson's correlation coefficient R measures the variance that is interpreted by the model, which is the reduction of variance when using the model. R values range from 0 to 1, however the model has healthy predictive ability when it is near to 1 and it is not predicting when near to 0. These performance metrics are a good measure of the overall predictive accuracy.

Furthermore, the following new engineering index, called a20-inex, has been proposed for the reliability assessment of the developed ANN models (Asteris *et al.* 2019, Asteris and Mokos 2020):

$$a10 - index = \frac{m10}{n} \tag{4}$$

where n is the number of dataset sample and m20 is the number of samples with value of rate Experimental value/Predicted value between 0.90 and 1.10. Note that for a perfect predictive model, the values of a10-index values are expected to be unity. The proposed a10-index has the advantage that their value has a physical engineering meaning. It declares the amount of the samples that satisfies predicted values with a margin ±10% compared to experimental values.

2.3 Database used for the training of ANN models

2.3.1 Need for reliable Data

During the training process of developing a mathematical model to predict a parameter value as a function of a number of other variables, most researchers tend to focus on computational aspects, while at the same time paying less attention to the database to be used for the training and development of the mathematical model.

However, the authors firmly believe that the main emphasis should be on the database to be used, as it is the database itself that describes the behavior of the problem to be modeled. The database, whether based on experimental or analytical data, is the available knowledge which must be properly utilized during the training process of the development of the mathematical model. In this regard, the database must be reliable with sufficient amount of data to adequately describe the problem under study.

It should be noted that the term "sufficient amount of data" does not necessarily imply a high amount of data, but rather datasets that cover a wide range of combinations of input parameter values, thus assisting in the model capability to simulate the problem. The demand for a reliable database is particularly crucial in the case of experimental databases, which are databases compiled using experimental results. In this case, significant deviations between experimental values are frequently noticed, not only between experiments conducted by different research teams and laboratories, but even between datasets derived from experiments conducted on specimens of the same synthesis, produced by the same technicians, cured under the same conditions, and tested implementing the same standards and testing instruments.

In light of the above discussion, for the training and development of the soft computing models for the prediction of the fire resistance of slim-floor steel beams an analytical database was compiled from FEM results.

In particular, an array of different types of slim-floor steel beams will be studied using the finite-element method, upon validating the FEM model used through simulating experimental data available in the literature.

2.3.2 Analytical data based on FEM

2.3.2.1 Analytical modeling

Finite element modelling for the unprotected slim floor beams is performed using the two-phase method explained and presented by Maraveas *et al.* 2012. In the initial phase, temperature contours for the slim floors are obtained by performing the thermal analysis. The convection coefficients for exposed and unexposed surfaces are taken equal to 25W/m^{2}K and 9 W/m^{2}K, respectively. The radiation emissivity for the bottom steel flange and the composite floor is taken as 0.7 following the EN1994-1-2 recommendations. Both concrete and steel are modelled using the 8-node linear brick elements, DC3D8 and the interface between the steel and the concrete is modelled as a perfect thermal contact allowing full heat transfer. Thermal analyses are performed for the standard fire exposure conditions (ISO 834 1999). This phase provides the thermal contours on the asymmetric slim floor beams.

The second phase of the numerical modelling consists of the thermomechanical analysis and is performed in two steps. During the first step, external loads, representing the degree of utilization of slim floor are applied while in the second step, the specimens are heated using the thermal contours obtained during the first phase. The external loads applied were uniformly distributed along the length of each beam. The concrete part is modelled using 8-node linear brick elements (C3D8) considering the numerical instabilities associated with the inelastic behaviour of concrete. On the other hand, the steel parts are modelled using hexahedral elements with reduced integration (C3D8R).

2.3.2.2 Validation against fire test results

The used numerical simulation procedure have been developed by Maraveas *et al.* 2012, and used successfully for number of similar simulations (Alam *et al.* 2021a, Alam *et al.* 2021b, Alam *et al.* 2018a, Alam *et al.* 2018b, Alam *et al.* 2018c, Alam *et al.* 2018d, Alam *et al.* 2019, Maraveas *et al.* 2014, Maraveas *et al.* 2017a, Maraveas *et al.* 2017b, Maraveas *et al.* 2017c). The used methodology is validated against experimental (fire test) results in Maraveas *et al.* 2012, Alam *et al.* 2021b and Alam *et al.* 2018a.

The slim floor cross section used in this research is similar to the cross section used during a fire test of a simply supported beam with span 4,0 m presented by Walnman 1996. Fig. 3(a) shows the cross section of the tested slim floor beam and Fig. 3(b) shows the position and numbering of thermocouples at mid-span cross section. The experiment simulated according the proposed methodology and results in terms of temperatures and mid-span deflection are showed in Fig. 4 and Fig. 5 respectively, showing good agreement between analytical modelling and experimental results.

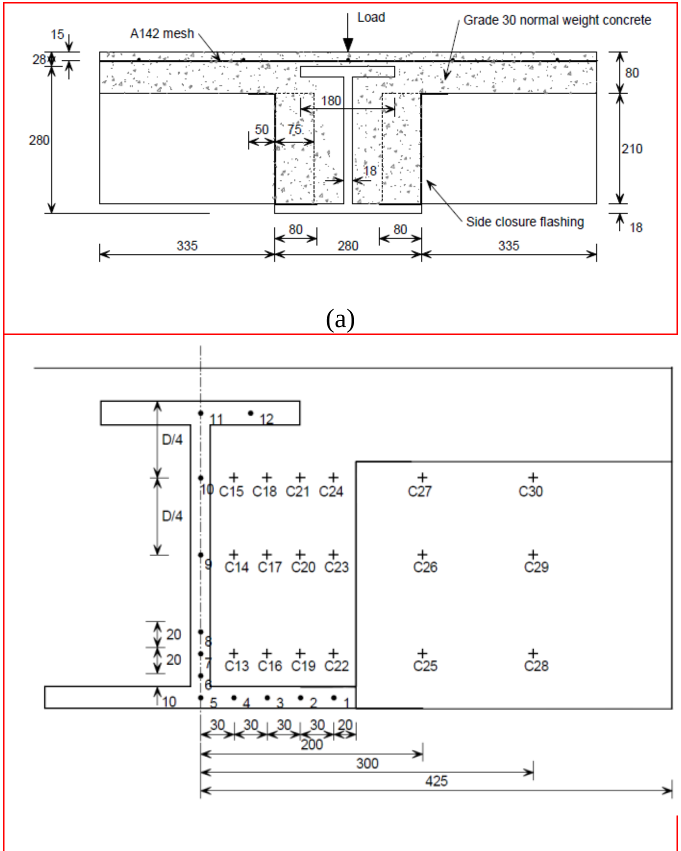

Fig. 3 Experimental setup: (a) Cross section of tested beam and (b) positions and numbering of thermocouples at the mid-span section (Walnman 1996)

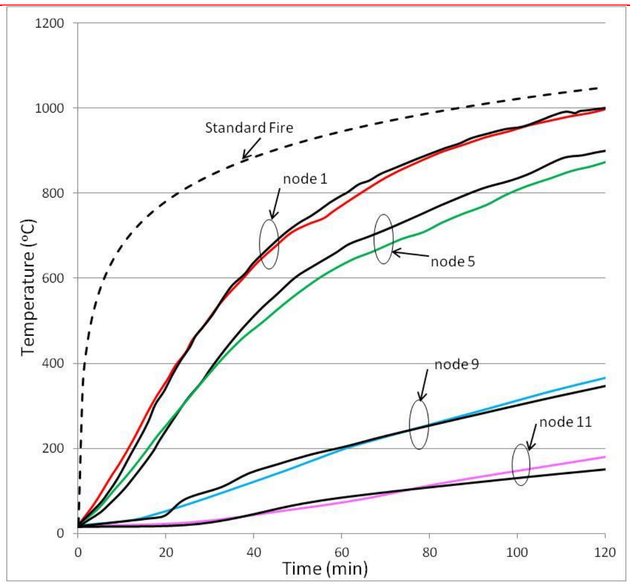

Fig. 4 Temperature histories from finite element analysis compared to experimental results (black curves show experimental results, colour curves show finite element analysis results).

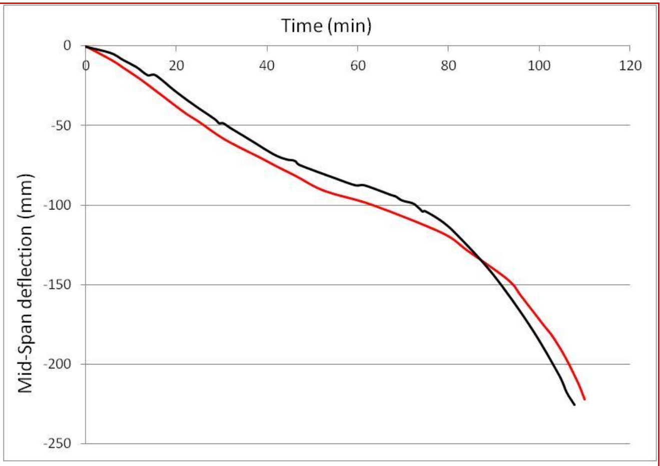

Fig. 5 Mid-span deflection, numerical vs experimental results (black curves show experimental results, colour curves show finite element analysis results).

2.3.2.3 Load factor

According EN1994-1-2 (2009), the design loads for the fire situation are given by the equation:

$$E_{fi,d} = n_{fi} E_d \tag{5}$$

where E_d is the design value of the corresponding force for a fundamental combination of actions, $E_{fi,d}$ is the design forces for fire design and n_{fi} is the reduction factor of E_d or called for simplicity as load factor. The load factor n_{fi} is a function of the reduction factor ψ_{fi} ($\psi_{1,1}$ or $\psi_{2,1}$) and of the ratio $Q_{k,1}/G_k$ and practically can take values between 0.75 and 0.25. EN1994-1-2 (2009) (Fig. 6). In this research, values from 0.37 and up to 0.85 have been considered.

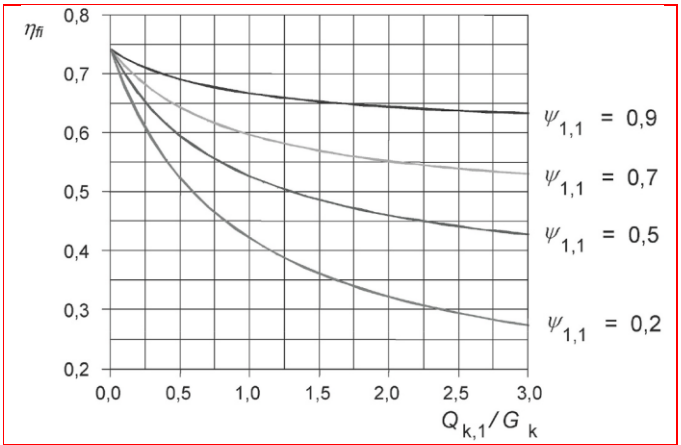

Fig. 6 Reduction factor of the design value of the corresponding force for a fundamental combination of actions n_{fi} as a function of the ratio $Q_{k,1}/G_k$ and $\psi_{1,1}$ (EN1994-1-2 2009)

2.3.2.4 Fire resistance

The simulations conducted under various degrees of utilization are representing potential fire tests. Hence, the fire resistance is defined and analyzed as done for fire tests.

The British Standards, BS 476–20 1987, provide the failure criteria in terms of the maximum mid-span deflection and the maximum rate of mid-span deflection. According to BS 476–20 1987, the failure is deemed to occur when the limits provided in Eqn. (6) and Eqn. (7) are exceeded. The units of the deflection in Eqn. (6) are in mm, while the units of rate of defection in Eqn. (7) are in mm/minute. It should be noted that the failure criterion in Eqn. (6) is only applicable when the deflection exceeds L/30. Similar performance criteria are also recommended by ASTM E119 2016.

$$L/20 \quad (6)$$

$$L^2/9000d \quad (7)$$

where, L is the clear span of the load-bearing horizontal element, in mm: d is the depth of the element, the distance from top to the bottom, in mm.

2.3.2.5 Undertaken analyses

The finite element analysis is performed for a slim floor beam of the cross section shown in Fig. 3(b). Four parameters were investigated including the span length, steel strength, concrete strength and the degree of utilization. The span lengths investigated were 4.5 m, 5.0 m, 5.5 m, and 6 m. The yield strength of steel was taken as 235 MPa, 275 MPa, 355 MPa, and 420 MPa, while the concrete's strength considered during the investigation was 25 MPa, 30 MPa, 35 MPa, and 40 MPa. The load factor was taken as 0.43, 0.48, 0.52 and 0.56 for the slim floor beam with span 4m, S355 and C30/37. When the span was increased the load was reduced to keep the applied moment constant. When the moment capacity was changing due to different applied steel or concrete grades, the new load factor was calculated, keeping the applied load constant.

2.3.3 Statistical indices of database

Following the above, a detailed database was created consisting of 256 datasets. Each dataset consists of five parameters, of which the input parameters are the length of the beam, the load factor, the steel yield strength and the concrete compressive strength, while the output parameter is the fire resistance of slim-floor steel beams.

Table 1 reports a brief statistical analysis for all the datasets in the database, considering each input and output variable individually and presenting minimums, maximums, averages, and standard deviation.

The correlation between all input and output variables in the database is revealed in Table 2 using the Pearson correlation coefficient R. In general, an R coefficient among input variables that approaches 1 or –1 indicates a strong linear relationship between them. The value of correlation factor between each input parameter and the output parameter indicates which one among the input parameters mainly affects the value of the predicted parameter, which herein is the fire resistance. Based on Table 2, the highest coefficient among input variables and output variable (bottom line), is –0.88, and corresponds to the load factor (LF). The second-highest correlation coefficient is 0.77, corresponds to steel yield strength (SYS). For all other cases, the correlation coefficient is quite lower.

Figures 7 to 11 show the histograms for each of the five parameters involved in the problem under study. These figures are particularly useful, as they define the range of values of the five parameters for which the proposed optimal mathematical model can be applied reliably. In addition, certain ranges of parameter values are specified for which the reliability of the mathematical model is expected to be unreliable. This happens when ranges of parameter values exist in which there is not enough data to properly train the model.

Table 1 The input and output parameters used in the development of BPNNs

Variable	Abreviation	Symbol	Units	Category	Data used in NN Models			
					Min	Average	Max	STD
Length of Beam	L	L	m	Input	4.50	5.25	6.00	0.56
Load Factor	LF	n_{fi}	-	Input	0.37	0.58	0.85	0.14
Steel Yield Strength	SYS	fy	MPa	Input	235.00	321.25	420.00	71.67
Concrete Compressive Strength	CCS	f'c	MPa	Input	25.00	32.50	40.00	5.60
Fire Resistance	FR	FR	min	Output	13.20	50.48	92.00	16.28

Table 2 Correlation matrix of the input and output variables

Variables		Input				Output
		L	LF	SYS	CCS	FR
Input	L	1.00				
	LF	0.00	1.00			
	SYS	0.00	-0.90	1.00		
	CCS	0.00	0.00	0.00	1.00	
Output	FR	-0.28	-0.88	0.77	0.15	1.00

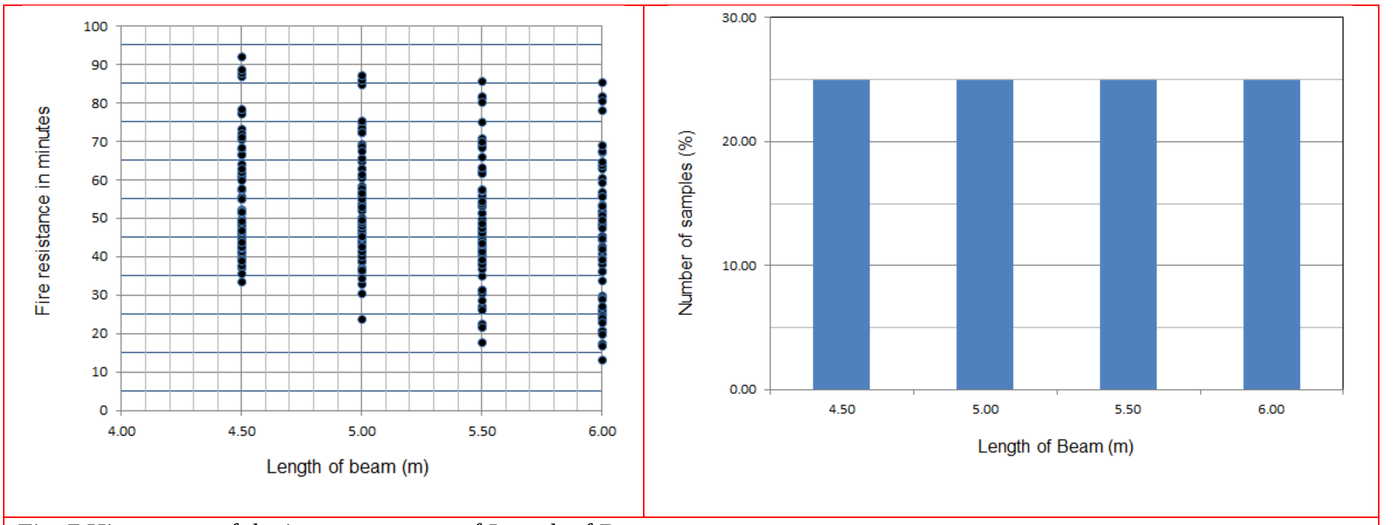

Fig. 7 Histograms of the input parameter of Length of Beam

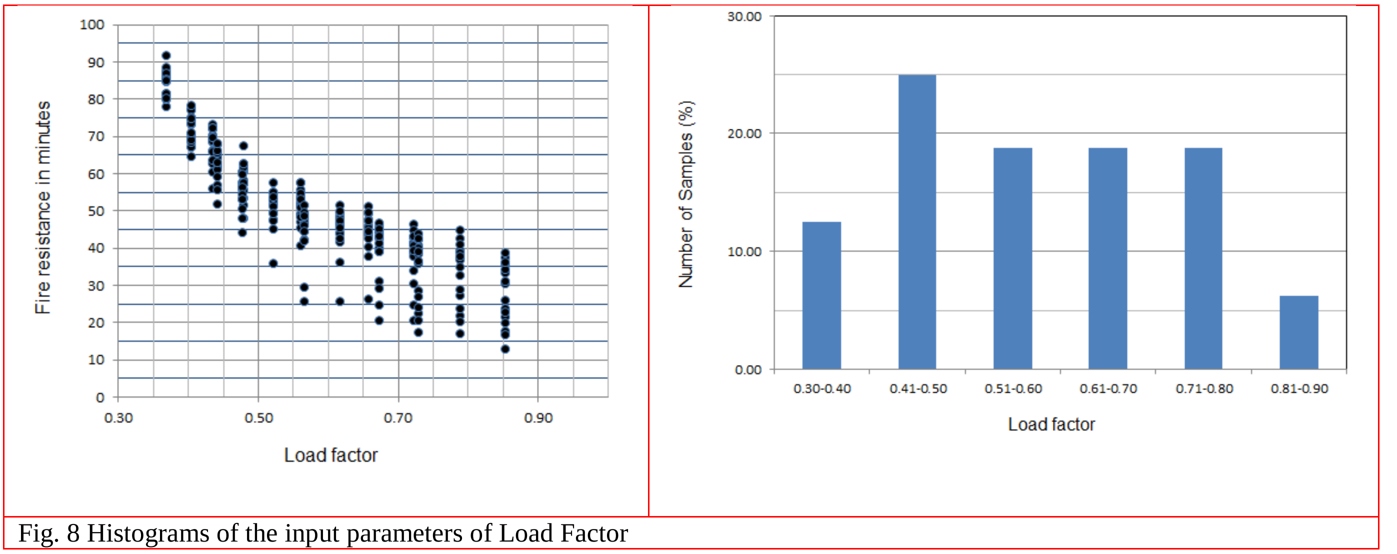

Fig. 8 Histograms of the input parameters of Load Factor

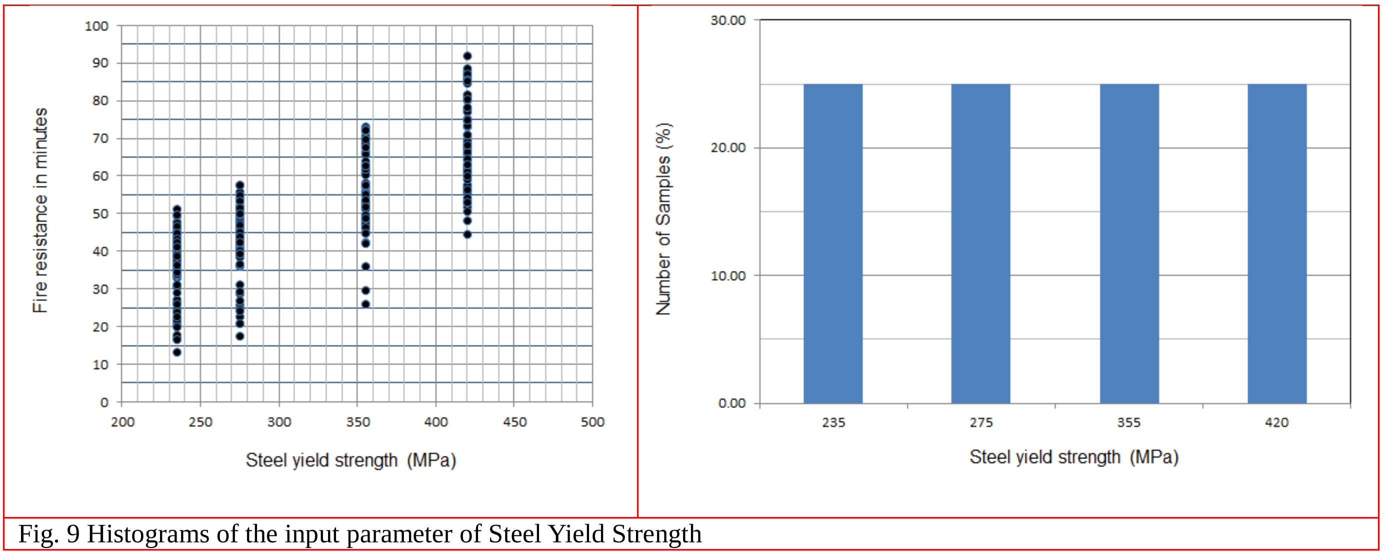

Fig. 9 Histograms of the input parameter of Steel Yield Strength

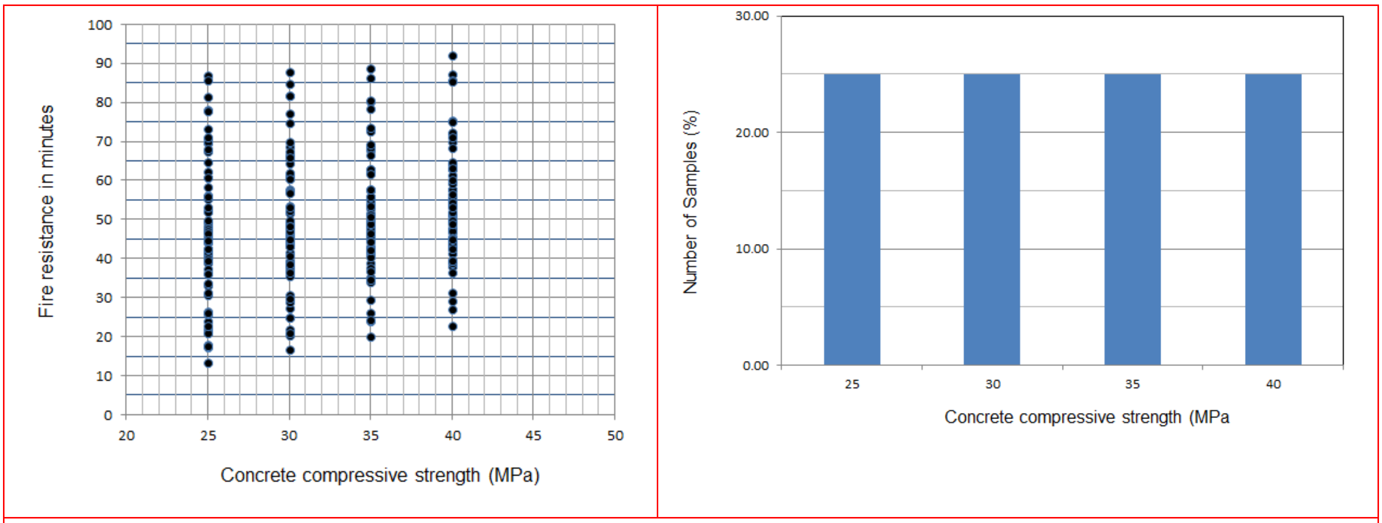

Fig. 10 Histograms of the input parameters of Concrete Compressive Strength

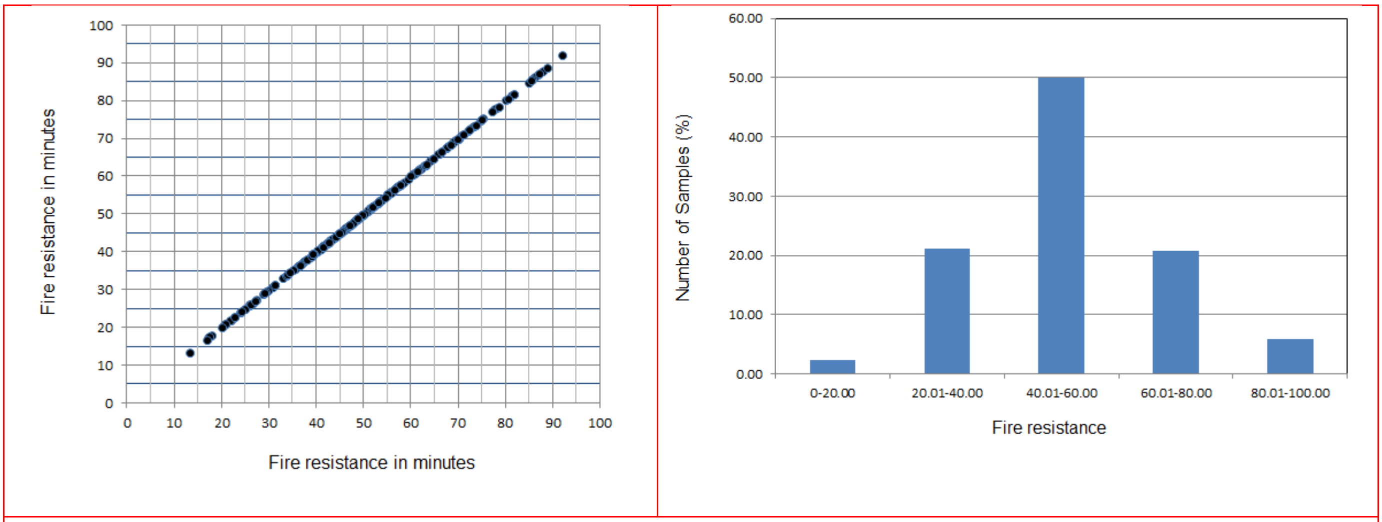

Fig. 11 Histograms of the output parameter of Fire Resistance

2.4 Sensitivity Analysis of Fire Resistance

It is especially important during the process of training and development of a computer model in order to predict the value of a parameter as a function of a series of other parameters affecting that parameter, to know which among them are the most important parameters. In fact, it is required to quantify the influence of each of these parameters so as to select the optimal number/combination of them in order to formulate the optimal computational mathematical simulation. In this regard, sensitivity analysis techniques on the predicted (output) parameter can be employed.

In general, sensitivity analysis (SA) of a numerical model is a technique used to determine if the output of the model is affected by changes in the input parameters. This provides feedback regarding which input parameters are the most significant, and thus, by removing the insignificant ones, the input space will be reduced and subsequently the complexity of the model, as well as the time required for its training, will be also reduced. In order to identify the effects of model inputs on the outputs, the SA can be conducted on the database. Sometimes, the results of SA help researchers/designers to remove one or more input parameters from the database to obtain better analyses with a higher level of performance prediction. To perform the SA, the cosine amplitude method (CAM) is employed, which has been used by many researchers (Armaghani and Asteris 2021, Armaghani *et al.* 2015, 2020, Momeni *et al.* 2015, Asteris *et al.* 2021). In CAM, data pairs may be used to construct a data array, X, as follows:

$$X = \{x_1, x_2, x_3, \ldots, x_i, \ldots, x_n\} \tag{8}$$

Variable x_i in array, X, is a length vector of m as:

$$x_i = \{x_{i1}, x_{i2}, x_{i3}, \ldots, x_{im}\} \tag{9}$$

The relationship between R_{ij} (strength of the relation) and datasets of X_i and X_j is presented by the following equation:

$$R_{ij} = \frac{\sum_{k=1}^{m} x_{ik} x_{jk}}{\sqrt{\sum_{k=1}^{m} x^2{}_{ik} \sum_{k=1}^{m} x^2{}_{ik}}} \quad (10)$$

The R_{ij} values between the Fire Resistance of Slim-floor Steel Beams and the input parameters are shown in Fig. 12. This analysis in accordance with correlation matrix of the input and output parameters presented in a previous section, reveals that, the concrete and steel mechanical parameters crucial affect the fire resistance of steel beams. Specifically, the steel yield strength and the concrete compressive strength have the greatest influence on fire resistance values, with strength values of 0.98 and 0.94 respectively, followed by the length of beams (0.937. The parameter with the lowest influence on fire resistance seems to be the load factor with a strength value of 0.86.

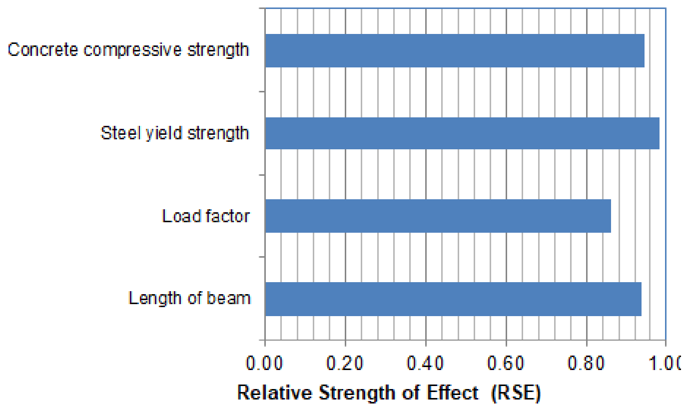

Fig. 12 Fire Resistance Sensitivity analysis of Slim-floor Steel Beams

3. Results and discussion

3.1. Development of ANN models

Based on the above, different architecture ANNs were developed and trained. More specifically, during the development and training of the ANN models the following steps (which are summarized in Table 3) were followed:

- The 256 datasets in the database, used for the training and development of the ANN models, were divided into three separate sets. Specifically, 171 of 256 (66.80%) datasets were designated as Training datasets, 42 (16.418%) as Validation datasets, while 43 (16.80%) datasets were used as Testing datasets.
- During the training of the ANNs, the above datasets were used with and without normalization. When normalization of the data was conducted, the minmax normalization technique in the range [0.10, 0.90] and [-1.00, 100) as well as the Zscore were implemented.
- The Levenberg–Marquardt algorithm (Lourakis 2005) was used for the training of the ANNs.
- 10 different initial values of weights and biases were applied for each architecture (Table 6).
- ANNs with only one hidden layer were developed and trained.
- The Number of Neurons per Hidden Layer ranged from 1 to 30, by an increment step of 1.
- Two functions, the Mean Square Error (MSE) and Sum Square Error (SSE) functions were used as cost functions, during the training and validation process.
- 10 functions, as presented in Table 6, were used as transfer or activation functions

The above steps resulted in the development of 240.000 different ANNs. It is worth noting that only the use of 10 different transfer function results in 100 different ANNs, for each architecture with the same number of neurons, as a result of 100 (=10^2) different dual combinations of the 10 transfer functions investigated.

3.2. Optimum ANN model

The above developed 240.000 ANNs were ranked based on the value of the RMSE performance index, for the case of Testing Datasets, and the top 20 architectures are presented in Table 4. Among them, the optimum ANN model, based on the value of RMSE of Testing Datasets, is the BPNN 4-9-1 model. The optimum model utilizes for data normalization the MinMax function, which converts the input and output values within the [0.10, 0.90] range. Also, it employs the Hyperbolic Tangent Sigmoid transfer function (HTS) for the input layer and Symmetric saturating linear transfer function (SSL) for the output layer, while its cost function is the Sum Square Error (MSE) function. Fig. 13, illustrates graphically the neuron layout and the overall architecture of the optimum, BPNN-4-9-1 model. In Table 5, the performance of the optimum model is presented, for both the training and testing datasets and in terms of all five performance indices. It is noted that the selected optimum model achieved the best performance, among all alternative architectures, for every one of the five indices. Its performance both for the training and testing datasets is expectedly improved, particularly in terms of a10-index, where it achieves 100% of the samples to match of the analytical values, within a ±10% margin.

In Figs. 14 and 15 the scatter plots of the analytical vs predicted values, by the optimum BPNN-4-9-1 model, are presented for the training and the testing datasets. In these diagrams, except for the diagonal line that indicates an ideal prediction, two more lines are drawn marking a ±10% error margin, which correspond to the limits defined by the a10-index. Also, the ratio of experimental to predicted values for the same datasets are shown in Figs. 14 and 15.

At this point, it is worth noting that among the 20 best architectures of the developed ANNs, as presented in Table 4, the dominant position regarding the normalization technique is held by Minmax in the range [0.1, 0.90] (15 of the 20 best architectures), followed by Minmax in the range [-1.00,1.00] (4 of the 20 best architectures), and finally Zscore normalization technique (1 of the 20 best architectures), which is in fact ranked in 14th place. The top 20 architectures for each of the four normalization techniques used are presented in Tables A2 to A5 of the appendix.

Table 3. Training parameters of ANN models

Parameter	Value	Matlab function
Training Algorithm	Levenberg-Marquardt Algorithm	trainlm
Normalization	Minmax in the range [0.10 – 0.90] and [-1.00-1.00] Zscore	Mapminmax zscore
Number of Hidden Layers	1	
Number of Neurons per Hidden Layer	1 to 30 by step 1	
Control random number generation	10 different random generation	rand(seed, generator), where generator range from 1 to 10 by step 1
Epochs	200	
Cost Function	Mean Square Error (MSE) Sum Square Error (SSE)	mse sse
Transfer Functions	Hyperbolic Tangent Sigmoid transfer function (HTS) Log-sigmoid transfer function (LS) Linear transfer function (Li) Positive linear transfer function (PLi) Symmetric saturating linear transfer function (SSL) Soft max transfer function (SM) Competitive transfer function (Co) Triangular basis transfer function (TB) Radial basis transfer function (RB) Normalized radial basis transfer function (NRB)	tansig logsig purelin poslin satlins softmax compet tribas radbas radbasn

Table 4. Best twenty optimum architectures of ANN models based on Testing datasets RMSE index

Ranking	Normalization Technique	Cost Function	Transfer Function		Architecture	Epochs	Datasets	
							Testing	
			Input Layer	Output Layer			R	RMSE
1	Minmax [0.10, 0.90]	'SSE'	tansig	satlins	4-9-1	100	0.9981	0.9502
2	Minmax [-1.00, 1.00]	SSE	logsig	satlins	4-5-1	81	0.9981	0.9547
3	Minmax [0.10, 0.90]	SSE	tansig	satlins	4-4-1	100	0.9981	0.9776
4	Minmax [-1.00, 1.00]	MSE	tansig	tansig	4-5-1	81	0.9980	0.9941
5	Minmax [0.10, 0.90]	MSE	logsig	tansig	4-7-1	84	0.9978	1.0299
6	Minmax [0.10, 0.90]	MSE	tansig	logsig	4-6-1	84	0.9979	1.0313
7	Minmax [0.10, 0.90]	SSE	logsig	logsig	4-6-1	84	0.9979	1.0444
8	Minmax [0.10, 0.90]	SSE	logsig	satlins	4-9-1	84	0.9978	1.0472
9	Minmax [0.10, 0.90]	MSE	tansig	tansig	4-6-1	100	0.9977	1.0485
10	Minmax [0.10, 0.90]	MSE	logsig	satlins	4-10-1	84	0.9978	1.0493
11	Minmax [0.10, 0.90]	SSE	logsig	purelin	4-10-1	100	0.9977	1.0537
12	Minmax [-1.00, 1.00]	SSE	tansig	tansig	4-6-1	81	0.9977	1.0537
13	Minmax [0.10, 0.90]	MSE	logsig	poslin	4-7-1	100	0.9978	1.0555
14	Zscore	SSE	tansig	purelin	4-9-1	18	0.9977	1.0571
15	Minmax [-1.00, 1.00]	MSE	tansig	tansig	4-4-1	81	0.9977	1.0577
16	Minmax [0.10, 0.90]	SSE	logsig	logsig	4-6-1	100	0.9977	1.0607
17	Minmax [0.10, 0.90]	SSE	tansig	poslin	4-7-1	100	0.9977	1.0629
18	Minmax [0.10, 0.90]	MSE	logsig	tansig	4-7-1	84	0.9977	1.0630
19	Minmax [0.10, 0.90]	SSE	logsig	purelin	4-4-1	100	0.9977	1.0646
20	Minmax [0.10, 0.90]	SSE	logsig	poslin	4-4-1	100	0.9977	1.0646

Table 5. Summary of prediction capability of the optimum BPNN 4-9-1 model against existing methodologies

	Model	Datasets	Performance Indices				
			a10-index	R	RMSE	MAPE	VAF
1	BPNN 4-9-1	Training	1.0000	0.9968	1.3139	0.0167	99.3546
		Test	1.0000	0.9981	0.9502	0.0146	99.6178

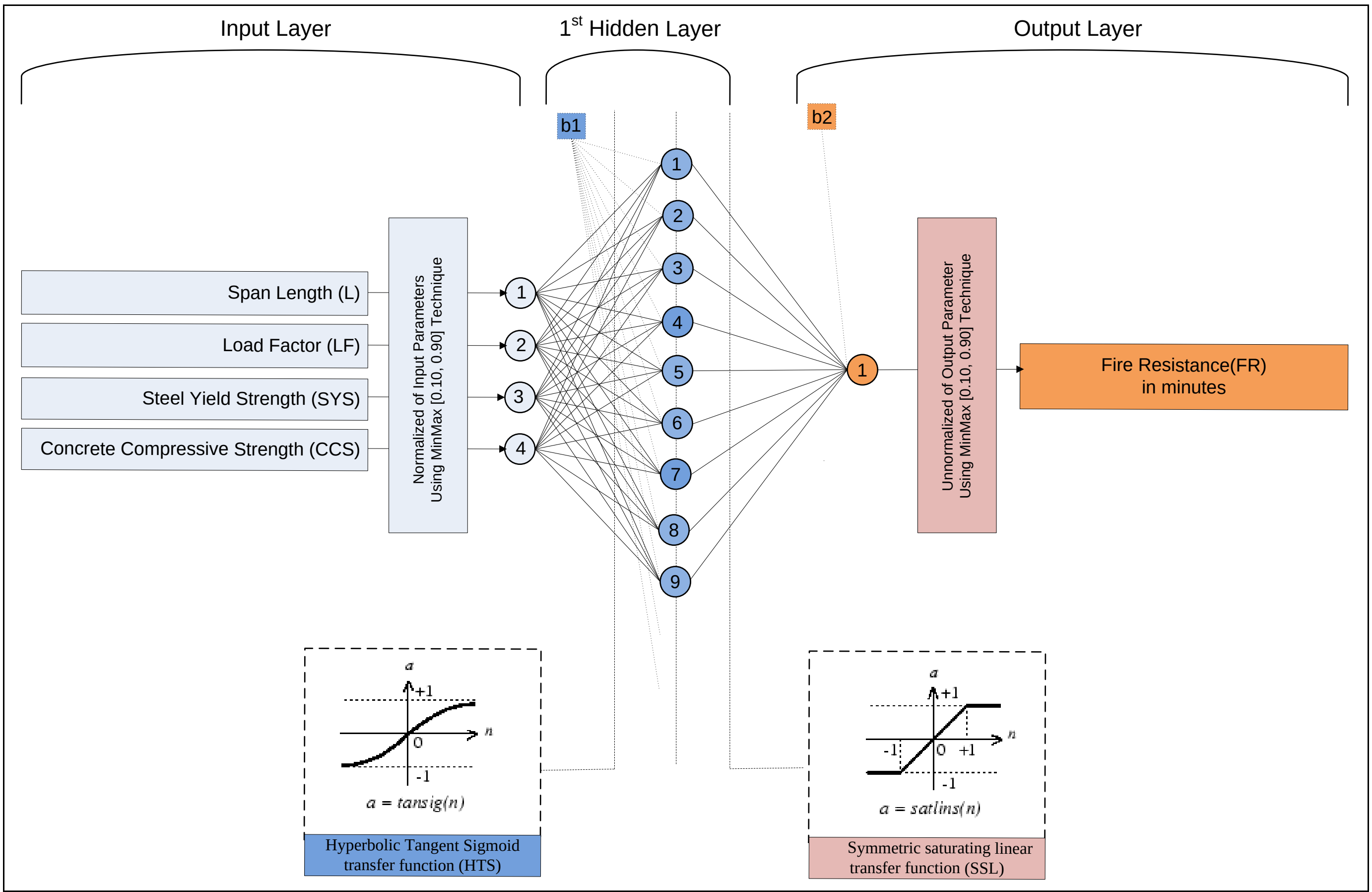

Fig. 13 Architecture of the optimum BPNN 4-9-1 model

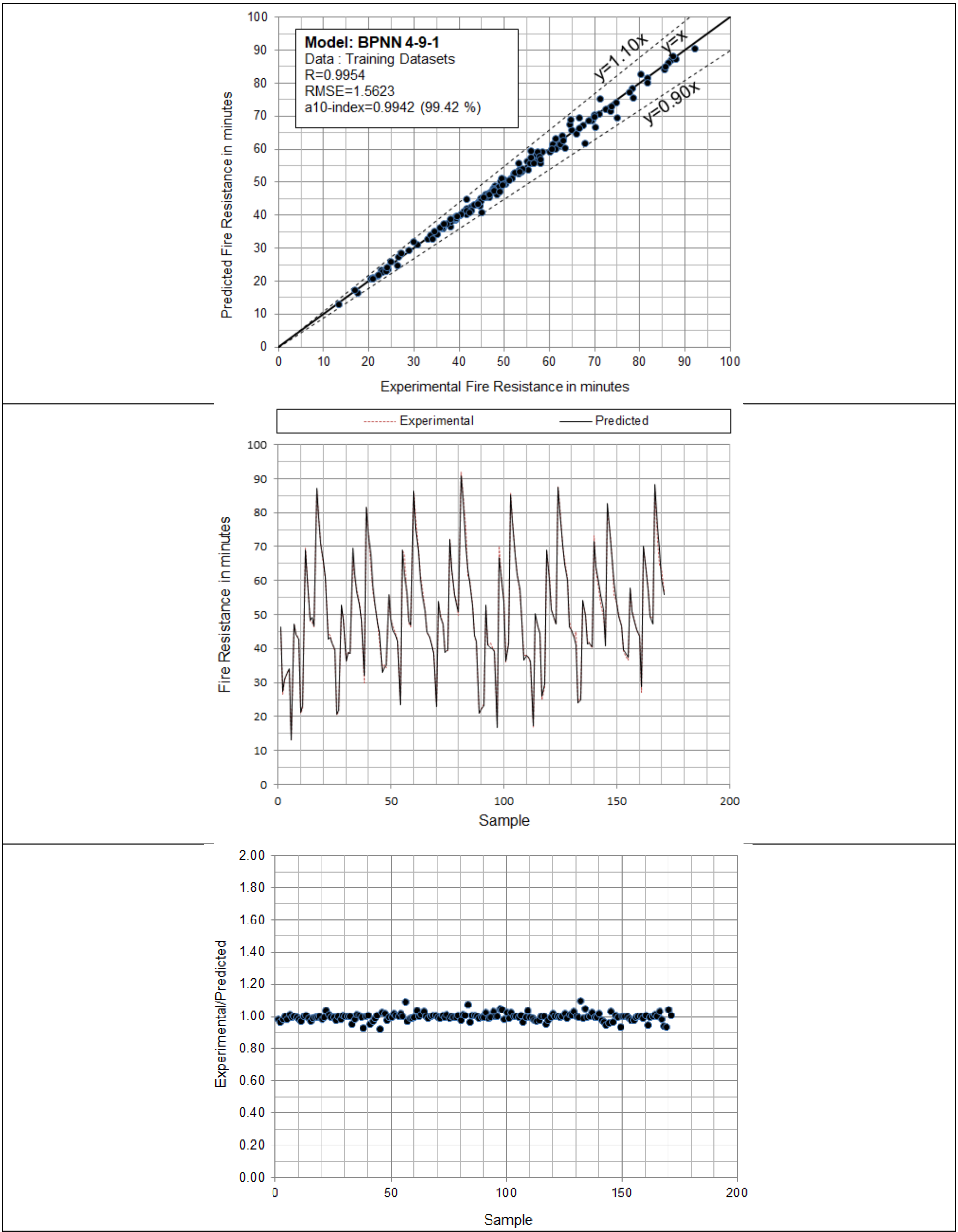

Fig. 14 Experimental vs predicted concrete compressive strength for Training datasets, using the developed BPNN-4-9-1 model.

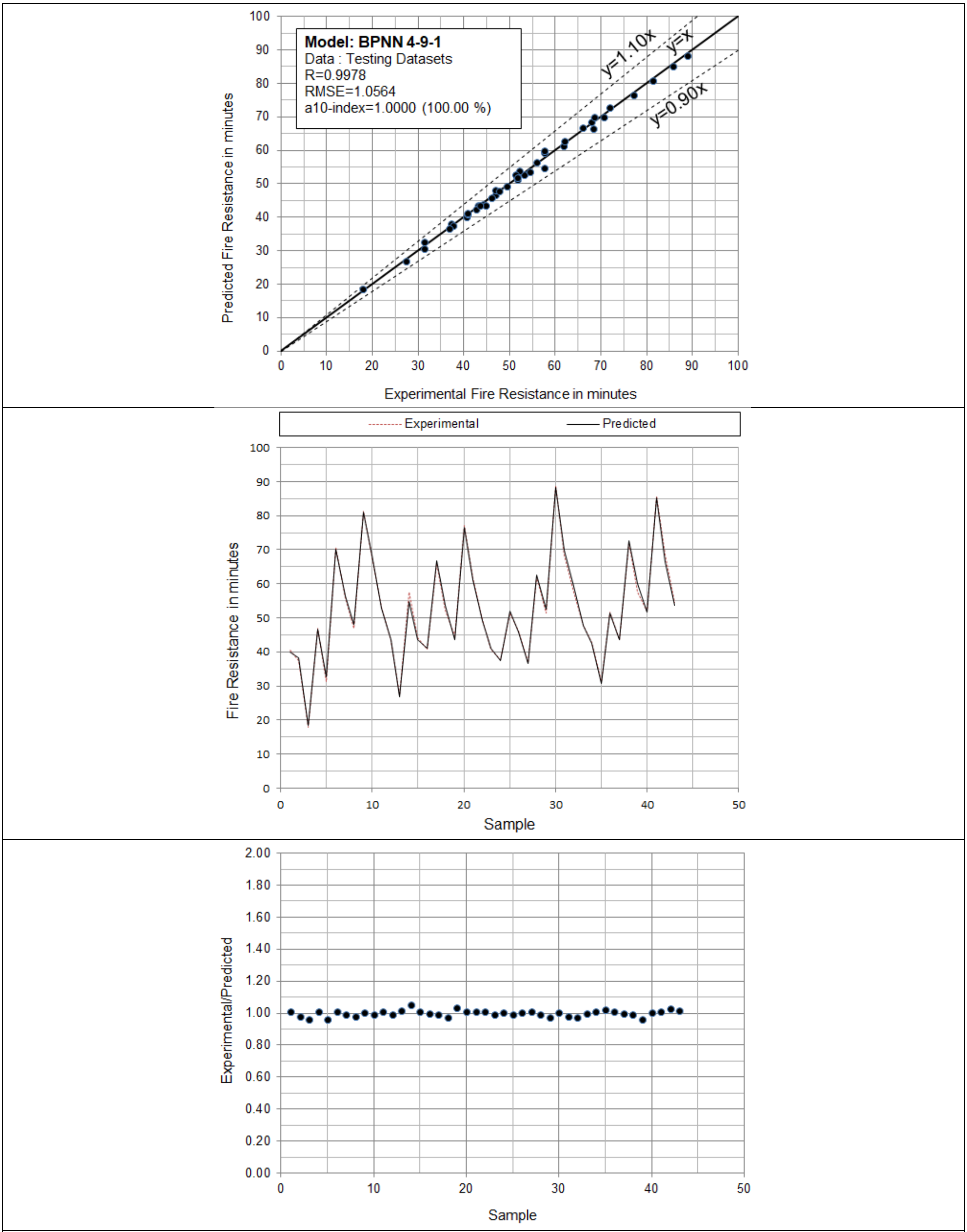

Fig. 15 Experimental vs predicted concrete compressive strength for Testing datasets, using the developed BPNN-4-9-1 model.

3.3. Closed form equation for the estimation of fire resistance based on the optimum ANN model

In a great number of research studies investigating the training and development of artificial neural networks, the final weights and biases of the ANN model are generally not reported. As a result, it becomes difficult, if not impossible, for other researchers or engineers in design practice, to implement the proposed model in their computers, reproduce the results or further improve upon it. To remove such an obstacle, this work presents the explicit mathematical equation, along with the values of weights and biases of our proposed model. Therefore, it can be readily implemented in a spreadsheet environment, by anyone interested, even without prior expertise in the field of Artificial Neural Networks.

The derived equation for the prediction of the fire resistance (FR) of slim-floor steel beams, using the length of beam (L), the load factor (LF), the steel yield strength (SYS) and the concrete compressive strength (CCS), is expressed by the following equation:

$$\mathrm{FR} = 98.50(\,\mathrm{tansig}([\mathrm{L_W}]\times[\mathrm{satlins}([\mathrm{I_W}]\times[\mathrm{IP}]+[\mathrm{b_i}])] + [\mathrm{b_0}]) - 0.10) + 13.20 \tag{11}$$

where satlins and tansig are the Symmetric saturating linear transfer function (SSL) and the Hyperbolic Tangent Sigmoid transfer function (HTS), respectively which are presented in details both their equations and graphs in Table A1 of the Appendix. $[\mathrm{I_W}]$ is a 9×4 matrix containing the weights of the hidden layer; $[\mathrm{L_W}]$ is a 1×9 vector containing the weights of the output layer; $[\mathrm{IP}]$ is a 4×1 vector with the 6 input variables, $[\mathrm{b_i}]$ is a 9×1 vector containing the bias of the hidden layer; and $[\mathrm{b_0}]$ is a 1×1 vector containing the bias of the output layer. Equation 8 describes the developed ANN model in a purely mathematical form, making it more accessible for engineers/researchers to use in practice.

The $[\mathrm{IP}]$ vector that contains the 4 normalized input variables (LB, LF, SYS and CCS) is expressed as:

$$[\mathrm{IP}] = \begin{bmatrix} 0.1 + 0.8\left(\dfrac{\mathrm{L} - 4.50}{1.5}\right) \\ 0.1 + 0.8\left(\dfrac{LF - 0.37}{0.48}\right) \\ 0.1 + 0.8\left(\dfrac{\mathrm{SYS} - 235}{185}\right) \\ 0.1 + 0.8\left(\dfrac{\mathrm{CCS} - 25}{15}\right) \end{bmatrix} \tag{12}$$

The above equation normalized the real values of the four input parameters using the minmax normalization technique in the range [0.10, 0.90]

The values of final weights and biases that determine matrices $[\mathrm{I_W}]$, $[\mathrm{L_W}]$, $[\mathrm{b_i}]$ and $[\mathrm{b_0}]$ are expressed by:

$$[\mathrm{I_W}] = \begin{bmatrix} -0.6237 & -0.1035 & 0.6121 & 0.5620 \\ 0.6215 & -1.1838 & 8.8462 & -0.5082 \\ -0.0268 & 1.8713 & 0.0038 & 0.0928 \\ 8.7540 & 16.1192 & 6.8662 & -4.2710 \\ -0.2488 & 2.5341 & -11.6123 & 8.0673 \\ 0.0100 & -21.1124 & -0.4000 & 0.6697 \\ -5.0755 & -2.4906 & -6.7115 & -0.3496 \\ 0.1277 & -6.1910 & 0.2944 & -0.2218 \\ -0.5299 & -2.0332 & -2.1176 & 1.9457 \end{bmatrix} \tag{13}$$

$$[\mathrm{L_W}]^{\mathrm{T}} = \begin{bmatrix} 1.8104 \\ -0.0415 \\ -0.8002 \\ -0.0511 \\ 0.0204 \\ 5.1046 \\ 0.0319 \\ 0.2102 \\ 0.3131 \end{bmatrix} \tag{14}$$

$$[\mathrm{b_i}] = \begin{bmatrix} 1.9905 \\ -1.7174 \\ 0.0551 \\ -16.8653 \\ 2.0195 \\ -0.4379 \\ 8.6494 \\ 7.1678 \\ -1.8636 \end{bmatrix} \tag{15}$$

and

$$[\mathrm{b_0}] = 4.4149 \tag{16}$$

3.4 Validation of the optimum ANN model regarding the overfitting problem

Although the statistical performance of the developed optimum model is always a matter deserving constant focus, it is also important to verify its prediction capacity employing engineering insight, and taking into account the expected physical behavior. Under this process it should be confirmed that no “overfitting” takes place, and that the model indeed approximates the governing laws of the problem in question (Armaghani and Asteris 2021). Thus, it was decided to conduct a verification of the optimal neural network, utilizing a selection of FEM analytical results. Specifically, in Figs. 16 to 19, the FEM analytical results are plotted against the respective curves predicted from the optimal neural network, for the same input parameters.

Figs. 16 to 19 clearly demonstrate that the proposed ANN model best fit the analytical FEM results. In addition, the smooth derived curves indicate that no overfitting problem takes place (in the case of overfitting the derived curves are characterized by curly shapes).

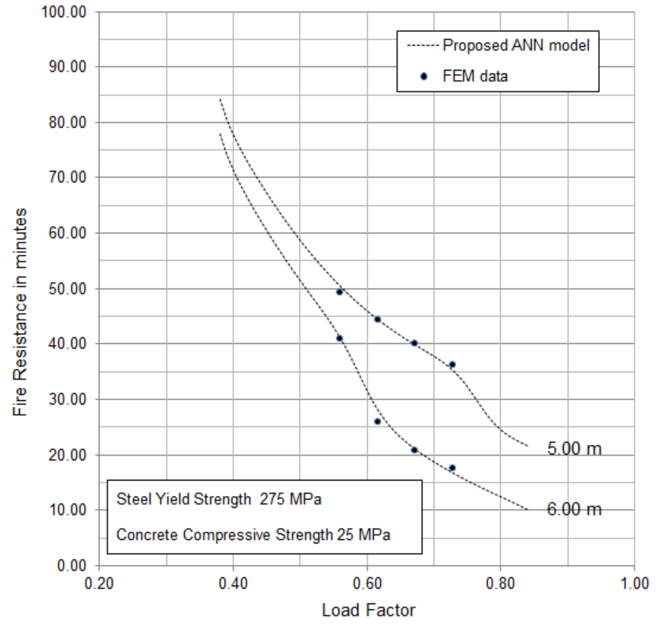

Fig. 16 Validation of the optimum BPNN 4-9-1 model with analytical FEM results for beam length 5.00 and 6.00 m while the yield compressive strength and concrete compressive strength are 275 and 25 MPa

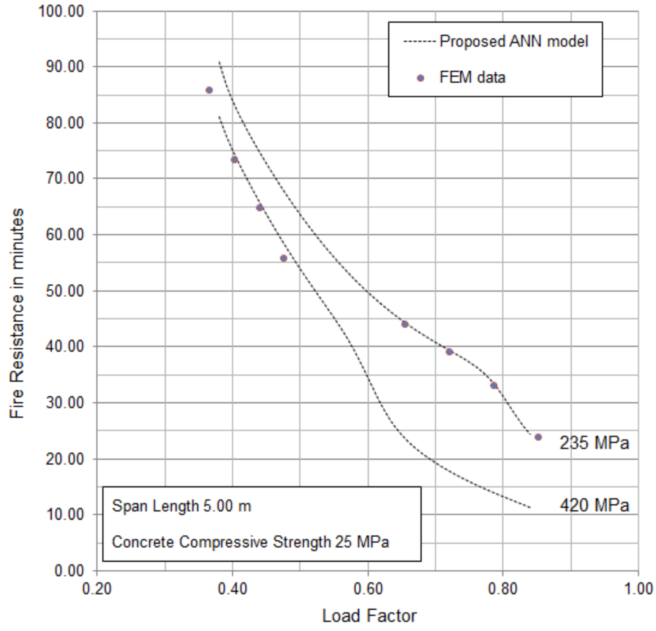

Fig. 18 Validation of the optimum BPNN 4-9-1 model with analytical FEM results for steel yield strength 235 and 420 MPa while the concrete compressive strength and the beam length are 25 MPa and 5 m respectively

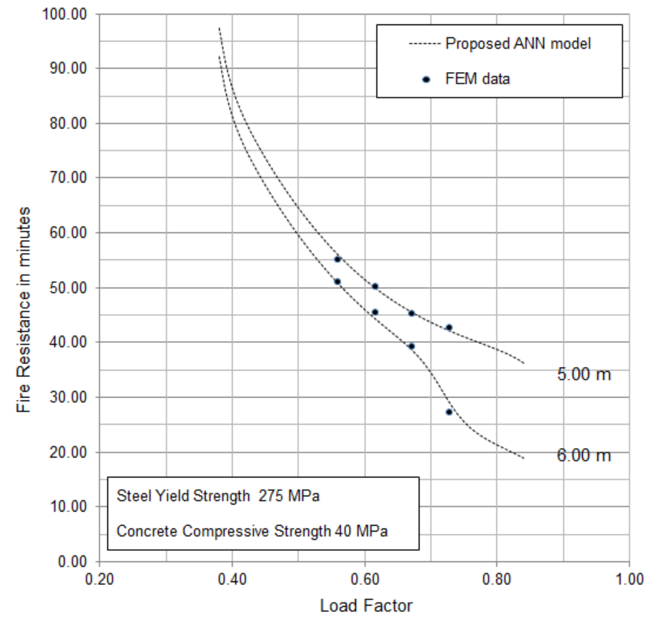

Fig. 17 Validation of the optimum BPNN 4-9-1 model with analytical FEM results for beam length 5.00 and 6.00 m while the yield compressive strength and concrete compressive strength are 275 and 40 MPa

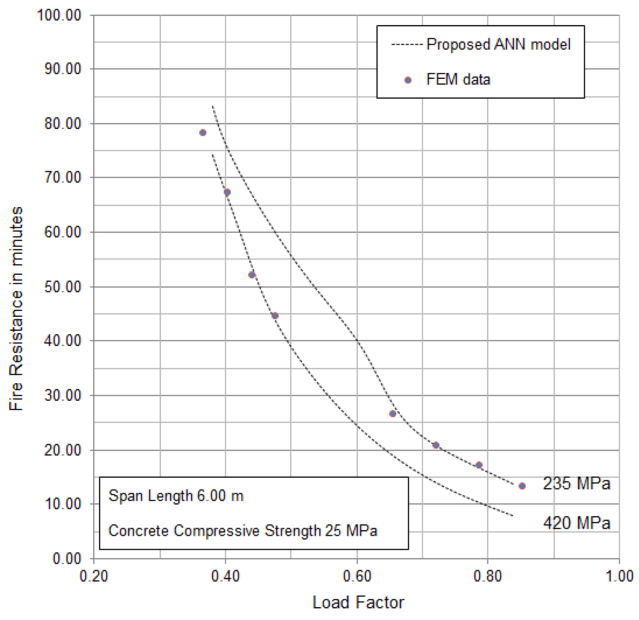

Fig. 19 Validation of the optimum BPNN 4-9-1 model with analytical FEM results for steel yield strength 235 and 420 MPa while the concrete compressive strength and the beam length are 25 MPa and 6 m respectively

Specifically, Fig. 16 presents the fire resistance predicted values of slim-floor steel beams for two different values of beam length 5.00 and 6.00 m respectively, while the yield compressive strength and concrete compressive strength are 275 and 25 MPa. Fig. 17 presents the fire resistance predicted values of slim-floor steel beams for two different values of beam length 5.00 and 6.00 m respectively, while the yield compressive strength and concrete compressive strength are 275 and 40 MPa. Fig. 18 presents the fire resistance predicted values of slim-floor steel beams for steel yield strength 235 and 420 MPa, while the concrete compressive strength and the beam length are 25 MPa and 5 m respectively. Finally, Fig. 19 presents the fire resistance predicted values of slim-floor steel beams for steel yield strength 235 and 420 MPa, while the concrete compressive strength and the beam length are 25 MPa and 6 m respectively.

Figs. 16 to 19 clearly demonstrate the strong nonlinear relation among the load factor and the fire resistance of slim-floor steel beams. Furthermore, for all presented cases, an increase of load factor results in a decrease of fire resistance. Fig. 16 and Fig. 17 show that an increase in beam span length yields a nonlinear decrease of fire resistance. The larger the load factor, the greater the reduction in fire resistance. An analogous remark holds for the quality of steel: an increase in the steel yield strength, yields a nonlinear decrease of fire resistance (Fig. 18 and Fig. 19). The larger the steel yield strength, the greater the reduction in fire resistance.

The optimal neural network, BPNN 4-9-1, exhibits excellent convergence to the experimental results, even though it was trained with only 66.7% of the database datasets. Overfitting, typically manifested with highly anomalous prediction curves, is avoided, since the obtained curves reveal a smooth interpolation of the concrete strength in the space between the experimental data.

Furthermore, based on the developed and presented optimum BPNN 4-9-1 model, a plethora of fire resistance curves can be obtained for different values combinations of the input parameters of steel beam length, load factor, steel yield strength, and concrete compressive strength.

3.5. Revealing the nonlinear nature of slim-floor steel beams fire resistance

The complexity of the prediction of the fire resistance of slim-floor steel beams is attributed to the nonlinear nature of this composite structure, regarding its fire resistance as a function of the geometrical and mechanical parameters. In order to highlight this complexity, and to demonstrate that the optimum ANN model developed herein can reproduce these phenomena, a relevant analysis has been undertaken, showcasing the model predictions in a number of typical value ranges of the input parameters. Specifically, in Fig. 20, six fire resistance contour maps, derived by the optimum BPNN 4-9-1 model, for three different steel yield strengths (235, 275 and 355 MPa) and two different concrete compressive strengths (20 and 40 MPa) are presented.

These contour maps clearly depict the nonlinear nature of this composite structural element. Fig. 20 (a) presents the fire resistance contour map for steel yield strengths of 235 MPa and concrete compressive strengths of 25 MPa. As shown in this figure, a highly nonlinear relation between the fire resistance of slim-floor steel beams and both the length of beam and the load factor is revealed, whereas the maximum fire resistance is attained for low values of load factor and low values of beam length. These observations are confirmed also in all six presented maps. Regarding the strength of concrete, it can be seen that an increase in concrete compressive strength leads to an increase in fire resistance (three left column maps that correspond to concrete compressive 25 MPa vs the three right column maps that correspond to concrete compressive 40 MPa).

All of the above demonstrates that the proposed mathematical model can reliably reveal the complex and highly nonlinear behavior of fire resistance of slim-floor steel beams as a function of the parameters involved in this problem. In addition, it presents a useful tool for the practicing engineer, while at the same time can effectively support the teaching of this subject at an academic level.

4. Conclusions

In the work presented herein, a new soft computing model for the fire resistance prediction of slim-floor asymmetric steel beams using single hidden layer was presented. The model is based on the ANN technique, employing a number of 30 neurons in a single hidden layer. Its development employed ten different activation functions and normalization techniques and it was selected as the optimum from 240000 alternative configurations tested and compared with several performance indices. The following points are the main conclusions from the development procedure:

- The proposed model predicts the fire resistance in a quite satisfactory manner offering 10% error margin for 100% of the specimens, both for testing and training datasets.
- For the optimum ANN model, it was found that the minmax normalization technique of the data in the range [0.10,0.90] provided better prediction capability compared to other normalization techniques used. Regarding transfer activation functions the Hyperbolic Tangent Sigmoid transfer function (HTS) proved more effective for the hidden layer, while the Symmetric saturating linear transfer function (SSL) was more effective for the output layer.
- According to the results from sensitivity analysis, among the several input variables, the most influencing one proved to be the steel yield strength, followed by the concrete compressive strength.
- Based on the optimum developed ANN model, a closed-form equation for the estimation of fire resistance is derived, which can prove a useful tool for researchers and engineers, while at the same time can effectively support the teaching of this subject at an academic level.

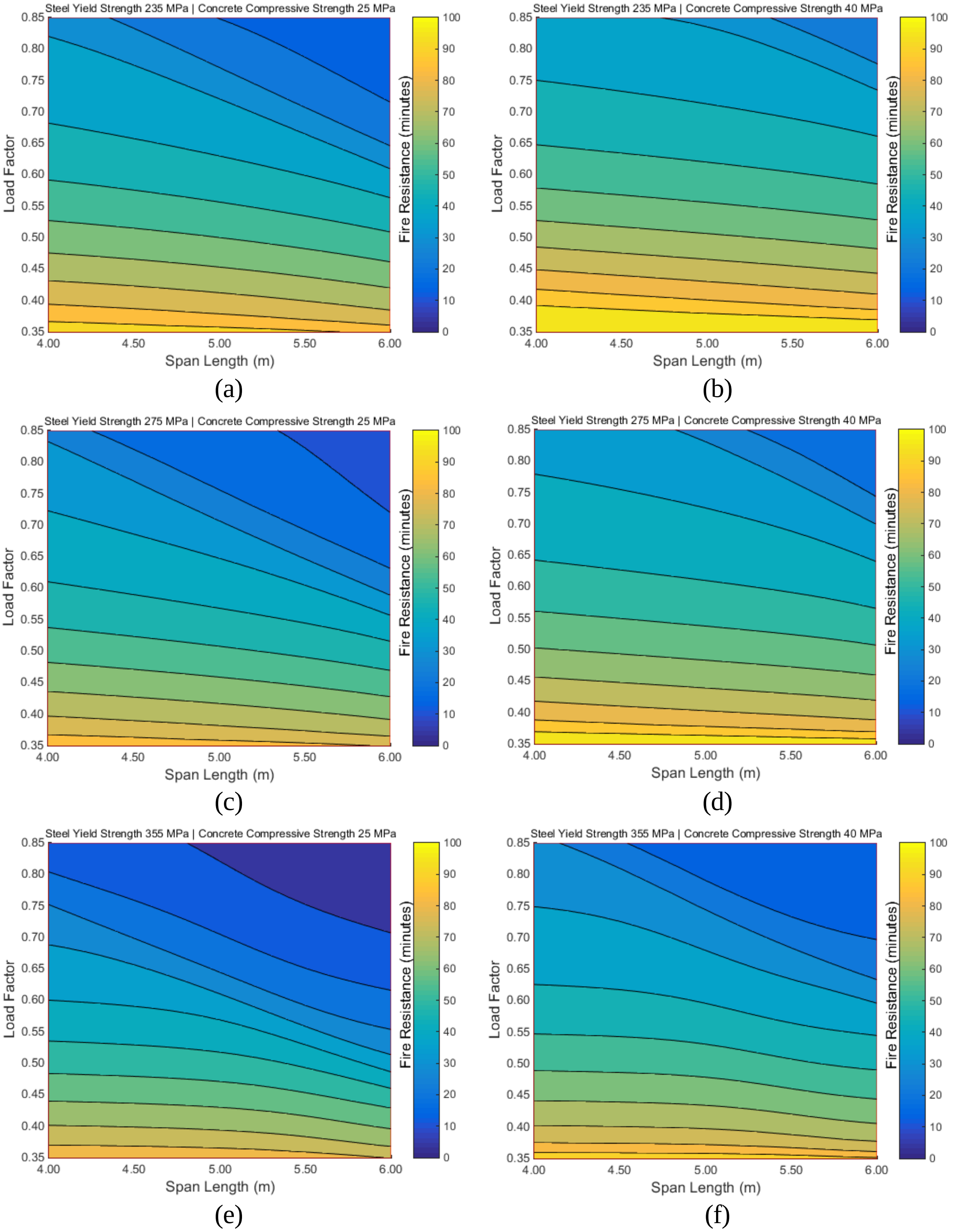

Fig. 20 Fire resistance contour maps for three different steel yield strengths (235, 275 and 355 MPa) and two different concrete compressive strengths (20 and 40 MPa).

- Furthermore, using the optimum developed and proposed ANN model, a first attempt has been undertaken producing maps in order to reveal the strongly nonlinear and complex mechanical behavior of these complex composite structures. Based on the derived maps, it seems that all these nonlinear phenomena can be totally revealed in a reliable and robust manner.

Despite the significant findings of the present study which demonstrate the effectiveness of the proposed ANN model and the associated closed-form equation for the fire resistance prediction of slim-floor asymmetric steel beams, it is deemed necessary to update and enrich the database with more data in order to develop a new mathematical model aiming at a holistic approach to the problem of fire resistance prediction, which significantly influences the design of these structures.

Appendix

Table A1. Tranfer functions of the optimum BPNN 4-9-1

Nr.	Tranfer Function/Equation/Matlab Function	Graph
1	Hyperbolic tangent sigmoid transfer function $a = f(n) = \frac{2}{1+\exp(-2*n)} - 1$ $a = f(n) = \text{tansig}\ (n)$	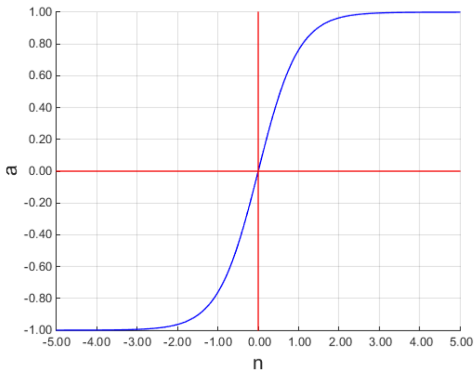
2	Symmetric saturating linear transfer function $a = f(n) = \begin{cases} -1, & n \leq -1 \\ n, & -1 < n < 1 \\ -1, & n \geq 1 \end{cases}$ $a = f(n) = \text{satlins}\ (n)$	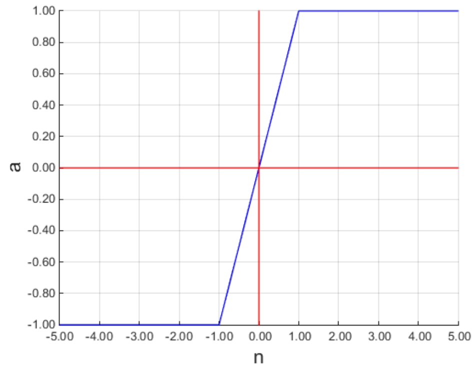

Table A2. Best twenty optimum architectures of ANN models based on Testing datasets RMSE index for the case without any normalization technique of datasets

Ranking	Normalization Technique	Cost Function	Transfer Function		Architecture	Epochs	Datasets	
							Testing	
			Input Layer	Output Layer			R	RMSE
1	Without Normalization	MSE	tansig	purelin	4-9-1	85	0.9977	1.0968
2	Without Normalization	MSE	tansig	poslin	4-28-1	85	0.9972	1.1578
3	Without Normalization	MSE	logsig	poslin	4-17-1	100	0.9972	1.1645
4	Without Normalization	MSE	logsig	purelin	4-24-1	100	0.9973	1.1659
5	Without Normalization	MSE	logsig	poslin	4-24-1	100	0.9973	1.1659
6	Without Normalization	MSE	tansig	poslin	4-30-1	93	0.9972	1.1814
7	Without Normalization	MSE	logsig	poslin	4-15-1	100	0.9971	1.1911
8	Without Normalization	MSE	logsig	purelin	4-18-1	99	0.9970	1.2038
9	Without Normalization	MSE	logsig	purelin	4-26-1	85	0.9970	1.2055

10	Without Normalization	SSE	tansig	poslin	4-20-1	85	0.9969	1.2171
11	Without Normalization	MSE	logsig	purelin	4-18-1	85	0.9968	1.2255
12	Without Normalization	MSE	tansig	poslin	4-27-1	99	0.9969	1.2260
13	Without Normalization	SSE	tansig	poslin	4-29-1	85	0.9968	1.2310
14	Without Normalization	MSE	logsig	purelin	4-18-1	100	0.9968	1.2425
15	Without Normalization	MSE	tansig	purelin	4-25-1	85	0.9967	1.2485
16	Without Normalization	MSE	tansig	purelin	4-21-1	100	0.9968	1.2506
17	Without Normalization	MSE	logsig	purelin	4-12-1	85	0.9967	1.2547
18	Without Normalization	MSE	logsig	purelin	4-9-1	93	0.9967	1.2600
19	Without Normalization	SSE	tansig	poslin	4-26-1	85	0.9968	1.2635
20	Without Normalization	MSE	logsig	purelin	4-14-1	85	0.9967	1.2653

Table A3. Best twenty optimum architectures of ANN models based on Testing datasets RMSE index for the case with Minmax [0.10, 0.90] normalization technique of datasets

Ranking	Normalization Technique	Cost Function	Transfer Function		Architecture	Epochs	Datasets	
							Testing	
			Input Layer	Output Layer			R	RMSE
1	Minmax [0.10, 0.90]	'SSE'	tansig	satlins	4-9-1	100	0.9981	0.9502
2	Minmax [0.10, 0.90]	SSE	tansig	satlins	4-4-1	100	0.9981	0.9776
3	Minmax [0.10, 0.90]	MSE	logsig	tansig	4-7-1	84	0.9978	1.0299
4	Minmax [0.10, 0.90]	MSE	tansig	logsig	4-6-1	84	0.9979	1.0313
5	Minmax [0.10, 0.90]	SSE	logsig	logsig	4-6-1	84	0.9979	1.0444
6	Minmax [0.10, 0.90]	SSE	logsig	satlins	4-9-1	84	0.9978	1.0472
7	Minmax [0.10, 0.90]	MSE	tansig	tansig	4-6-1	100	0.9977	1.0485
8	Minmax [0.10, 0.90]	MSE	logsig	satlins	4-10-1	84	0.9978	1.0493
9	Minmax [0.10, 0.90]	SSE	logsig	purelin	4-10-1	100	0.9977	1.0537
10	Minmax [0.10, 0.90]	MSE	logsig	poslin	4-7-1	100	0.9978	1.0555
11	Minmax [0.10, 0.90]	SSE	logsig	logsig	4-6-1	100	0.9977	1.0607
12	Minmax [0.10, 0.90]	SSE	tansig	poslin	4-7-1	100	0.9977	1.0629
13	Minmax [0.10, 0.90]	MSE	logsig	tansig	4-7-1	84	0.9977	1.0630
14	Minmax [0.10, 0.90]	SSE	logsig	purelin	4-4-1	100	0.9977	1.0646
15	Minmax [0.10, 0.90]	SSE	logsig	poslin	4-4-1	100	0.9977	1.0646
16	Minmax [0.10, 0.90]	MSE	tansig	tansig	4-4-1	100	0.9977	1.0702
17	Minmax [0.10, 0.90]	MSE	poslin	radbas	4-13-1	100	0.9976	1.0758
18	Minmax [0.10, 0.90]	MSE	logsig	purelin	4-7-1	100	0.9976	1.0761
19	Minmax [0.10, 0.90]	SSE	logsig	tansig	4-7-1	84	0.9975	1.0807
20	Minmax [0.10, 0.90]	MSE	logsig	satlins	4-4-1	100	0.9976	1.0818

Table A4. Best twenty optimum architectures of ANN models based on Testing datasets RMSE index for the case with Minmax [-1.00, 1.00] normalization technique of datasets

Ranking	Normalization Technique	Cost Function	Transfer Function		Architecture	Epochs	Datasets	
							Testing	
			Input Layer	Output Layer			R	RMSE
1	Minmax [-1.00, 1.00]	SSE	logsig	satlins	4-5-1	81	0.9981	0.9547
2	Minmax [-1.00, 1.00]	MSE	tansig	tansig	4-5-1	81	0.9980	0.9941

3	Minmax [-1.00, 1.00]	SSE	tansig	tansig	4-6-1	81	0.9977	1.0537
4	Minmax [-1.00, 1.00]	MSE	tansig	tansig	4-4-1	81	0.9977	1.0577
5	Minmax [-1.00, 1.00]	MSE	logsig	purelin	4-4-1	81	0.9978	1.0702
6	Minmax [-1.00, 1.00]	MSE	logsig	satlins	4-6-1	81	0.9976	1.0753
7	Minmax [-1.00, 1.00]	SSE	logsig	purelin	4-10-1	81	0.9976	1.0788
8	Minmax [-1.00, 1.00]	SSE	logsig	purelin	4-5-1	81	0.9977	1.0813
9	Minmax [-1.00, 1.00]	MSE	logsig	satlins	4-8-1	81	0.9975	1.0820
10	Minmax [-1.00, 1.00]	SSE	tansig	purelin	4-12-1	81	0.9975	1.0830
11	Minmax [-1.00, 1.00]	SSE	logsig	satlins	4-7-1	81	0.9975	1.0835
12	Minmax [-1.00, 1.00]	MSE	softmax	purelin	4-7-1	81	0.9975	1.0860
13	Minmax [-1.00, 1.00]	MSE	logsig	satlins	4-6-1	100	0.9976	1.0863
14	Minmax [-1.00, 1.00]	MSE	tansig	purelin	4-10-1	81	0.9975	1.0880
15	Minmax [-1.00, 1.00]	SSE	tansig	satlins	4-5-1	81	0.9975	1.0914
16	Minmax [-1.00, 1.00]	SSE	poslin	tansig	4-11-1	81	0.9975	1.0921
17	Minmax [-1.00, 1.00]	SSE	logsig	satlins	4-6-1	81	0.9976	1.0979
18	Minmax [-1.00, 1.00]	MSE	logsig	satlins	4-4-1	81	0.9976	1.0981
19	Minmax [-1.00, 1.00]	MSE	logsig	tansig	4-4-1	80	0.9975	1.0983
20	Minmax [-1.00, 1.00]	SSE	softmax	tansig	4-7-1	81	0.9974	1.1075

Table A5. Best twenty optimum architectures of ANN models based on Testing datasets RMSE index for the case with Zscore normalization technique of datasets

Ranking	Normalization Technique	Cost Function	Transfer Function		Architecture	Epochs	Datasets	
							Testing	
			Input Layer	Output Layer			R	RMSE
1	Zscore	SSE	tansig	purelin	4-9-1	18	0.9977	1.0571
2	Zscore	MSE	radbas	purelin	4-7-1	58	0.9977	1.0736
3	Zscore	MSE	logsig	purelin	4-5-1	100	0.9977	1.0741
4	Zscore	MSE	tansig	purelin	4-6-1	18	0.9976	1.0742
5	Zscore	MSE	softmax	purelin	4-7-1	100	0.9976	1.0770
6	Zscore	SSE	logsig	purelin	4-8-1	58	0.9976	1.0806
7	Zscore	MSE	tansig	purelin	4-7-1	87	0.9975	1.0929
8	Zscore	SSE	tansig	purelin	4-5-1	87	0.9974	1.1170
9	Zscore	SSE	logsig	purelin	4-5-1	18	0.9974	1.1173
10	Zscore	MSE	logsig	purelin	4-13-1	18	0.9974	1.1189
11	Zscore	MSE	logsig	purelin	4-6-1	58	0.9974	1.1230
12	Zscore	SSE	tansig	purelin	4-5-1	18	0.9974	1.1246
13	Zscore	MSE	tansig	purelin	4-5-1	58	0.9973	1.1281
14	Zscore	MSE	tansig	purelin	4-12-1	18	0.9973	1.1323
15	Zscore	MSE	softmax	purelin	4-9-1	100	0.9974	1.1343
16	Zscore	MSE	softmax	purelin	4-7-1	18	0.9973	1.1374
17	Zscore	MSE	tansig	purelin	4-8-1	58	0.9974	1.1463
18	Zscore	SSE	softmax	purelin	4-6-1	100	0.9972	1.1480
19	Zscore	SSE	logsig	purelin	4-6-1	58	0.9972	1.1510
20	Zscore	MSE	tansig	purelin	4-5-1	18	0.9972	1.1515

References

Akbar, H., Suryana, N. and Sahib, S. (2011). "Training neural networks using Clonal Selection Algorithm and Particle Swarm Optimization: A comparisons for 3D object recognition." *2011 11th International Conference on Hybrid Intelligent Systems (HIS)*. 692–697.

Ahmed I. M., Tsavdaridis K.D., (2019) "The evolution of composite flooring systems: applications, testing, modelling and eurocode design approaches", J. Constr. Steel Res., 155, 286-300, https://doi.org/10.1016/j.jcsr.2019.01.007

Ahn, J.K. and Lee, C.H. (2017), "Fire behavior and resistance of partially encased and slim-floor composite beams", J. Constr. Steel Res., 129 276-285. https://doi.org/10.1016/j.jcsr.2016.11.018.

Alam, N., Maraveas, C., Tsavdaridis, K.D. and Nadjai, A. (2021a), "Performance of Ultra Shallow Floor Beams (USFB) exposed to standard and natural fires", J. Build. Eng., 102192. https://doi.org/10.1016/j.jobe.2021.102192.

Alam N., Nadjai A., Hanus F., Kahanji C., Vassart O., (2021b), "Experimental and numerical investigations on slim floor beams exposed to fire", J. Build. Eng.,42, 102810, https://doi.org/10.1016/j.jobe.2021.102810.

Alam, N., Nadjai, A., Ali, F. and Nadjai, W. (2018a), "Structural response of unprotected and protected slim floors in fire", J. Constr. Steel Res., 142, 44-54. https://doi.org/10.1016/j.jcsr.2017.12.009.

Alam, N., Nadjai, A., Ali, F., Vassart, O. and Hanus, F. (2018b). "Experimental and Analytical Investigations on Thermal Performance of Slim Floor Beams with Web Openings in Fire", Proceedings of the 10th International Conference on Structures in Fire, Belfast, UK,

Alam, N., Nadjai, A., Maraveas, C., Tsavdaridis, K. and Ali, F. (2018c). "Effect of air-gap on performance of fabricated slim floor beams in fire", Proceedings of the 9th International Conference on Advances in Steel Structures, Hong-Kong, China, https://doi.org/10.18057/ICASS2018.xxx.

Alam, N., Nadjai, A., Maraveas, C., Tsarvdaridis, K. and Kahanji, C. (2019a), "Effect of air-gap on response of fabricated slim floor beams in fire", J. Struct. Fire Eng.. https://doi.org/10.1108/JSFE-04-2018-0011.

Alam, N., Nadjai, A., Maraveas, C., Tsavdaridis, K.D. and Ali, F. (2018d). "Response of Asymmetric Slim Floor Beams in Parametric-Fires", J. Phys. Conference Series, https://doi.org/10.1088/1742-6596/1107/3/032009.

Alam, N., Nadjai, A., Vassart, O. and Hanus, F. (2019), "A detailed investigation on thermal behaviour of slim floor beams with web openings at elevated temperatures", J. Struct. Fire Eng.

Albero, V., Espinós, A., Serra, E., Romero, M. and Hospitaler, A. (2019), "Numerical study on the flexural behaviour of slim-floor beams with hollow core slabs at elevated temperature", Eng. Struct., 180, 561-573. https://doi.org/10.1016/j.engstruct.2018.11.061.

Albero, V., Serra, E., Espinós, A., Romero, M.L. and Hospitaler, A. (2020), "Innovative solutions for enhancing the fire resistance of slim-floor beams: Thermal experiments", J. Constr. Steel Res., 165, 105897. https://doi.org/10.1016/j.jcsr.2019.105897.

Alavi, A.H. and Gandomi, A.H. (2012), "Energy-based numerical models for assessment of soil liquefaction", *Geoscience Frontiers*, **3**(4), 541-555. https://doi.org/10.1016/j.gsf.2011.12.008.

Apostolopoulou, M., Armaghani, D.J., Bakolas, A., Douvika, M.G., Moropoulou, A. and Asteris, P.G. (2019). "Compressive strength of natural hydraulic lime mortars using soft computing techniques." *Procedia Structural Integrity*, **17**, 914–923. https://doi.org/10.1016/j.prostr.2019.08.122.

Apostolopoulou, M., Asteris, P.G., Armaghani, D.J., Douvika, MG., Lourenço, P.B., Cavaleri, L., Bakolas, A. and Moropoulou, A. (2020). "Mapping and holistic design of natural hydraulic lime mortars", *Cement and Concrete Research*, **136**, 106167, https://doi.org/10.1016/j.cemconres.2020.106167

Aqil, M., Kita, I., Yano, A. and Nishiyama, S. (2007). "A comparative study of artificial neural networks and neuro-fuzzy in continuous modeling of the daily and hourly behaviour of runoff." *Journal of Hydrology*, **337**, 22-34. https://doi.org/10.1016/j.jhydrol.2007.01.013.

Armaghani, D.J., Hajihassani, M., Sohaei, H., Mohamad, E.T., Marto, A., Motaghedi, H. and Moghaddam, M.R. (2015), "Neuro-fuzzy technique to predict air-overpressure induced by blasting", *Arab. J. Geosci.*, **8**(12), 10937–10950. https://doi.org/10.1007/s12517-015-1984-3.

Armaghani, D.J., Momeni, E. and Asteris, P.G. (2020). "Application of group method of data handling technique in assessing deformation of rock mass", *Metaheuristic Computing and Applications*, **1**(1), 1-18. http://dx.doi.org/10.12989/mca.2020.1.1.001

Armaghani, D.J. and Asteris, P.G. (2021). "A comparative study of ANN and ANFIS models for the prediction of cement-based mortar materials compressive strength", Neural Computing and Applications, *Neural Computing and Applications*, **33**(9), 4501-4532, DOI: 10.1007/s00521-020-05244-4

Armaghani, D.J., Mamou, A., Maraveas, C., Roussis, P.C., Siorikis, V.G., Skentou, A.D. and Asteris, P.G. (2021). "Predicting the unconfined compressive strength of granite using only two non-destructive test indexes", *Geomechanics and Engineering*, **25**(4).

ASTM E119-16 (2016) (American Society for Testing and Materials), E119-16 – Standard Test Methods for Fire Tests of Building Construction and Materials.

Asteris, P.G., Ashrafian, A., Rezaie-Balf, M. (2019). Prediction of the Compressive Strength of Self-Compacting Concrete using Surrogate Models, Computers and Concrete, 24(2), 137-150.

Asteris, P.G., Apostolopoulou, M., Skentou, A.D. and Moropoulou, A. (2019). "Application of artificial neural networks for the prediction of the compressive strength of cement-based mortars." *Computers and Concrete*, **24**, 329–345. 10.12989/cac.2019.24.4.329

Asteris, P.G and Mokos, V.G. (2020). "Concrete Compressive Strength using Artificial Neural Networks", *Neural Computing and Applications*, **32**, 1807–11826, https://doi.org/10.1007/s00521-019-04663-2.

Asteris, P.G., Lemonis, M.E., Nguyen, T.-A., Le, H.V. and Pham, B.T. (2021a). "Soft computing-based estimation of ultimate axial load of rectangular concrete-filled steel tubes", *Steel and Composite Structures*, **39**(4) (2021) 471-491 DOI: https://doi.org/10.12989/scs.2021.39.4.471

Asteris, P.G., Skentou, A.D., Bardhan, A., Samui, P., Pilakoutas, K. (2021b). "Predicting concrete compressive strength using hybrid ensembling of surrogate machine learning models", *Cement and Concrete Research*, 2021, **145**, 106449, DOI: 10.1016/j.cemconres.2021.106449.

Asteris, P.G., Koopialipoor, M., Armaghani, D.J., Kotsonis, E.A., Lourenço, P.B. (2021c). Prediction of Cement-based Mortars Compressive Strength using Machine Learning Techniques, Neural Computing and Applications, https://doi.org/10.1007/s00521-021-06004-8.

Asteris, P.G., Skentou, A.D., Bardhan,A., Samui, P., Lourenço, P.B. (2021d). Soft computing techniques for the prediction of concrete compressive strength using Non-Destructive tests, Construction and Building Materials, **303**,124450,https://doi.org/10.1016/j.conbuildmat.2021.124450.

Bailey, C. (1999), "The behaviour of asymmetric slim floor steel beams in fire", J. Constr. Steel Res., 50(3), 235-257. https://doi.org/10.1016/S0143-974X(98)00247-8.

Bailey, C. (2003), "Large scale fire test on a composite slim-floor system", Steel Compos. Struct., 3(3), 153-168. https://doi.org/10.12989/scs.2003.3.3.153.

Battiti, R. (1992). "First- and Second-Order Methods for Learning: Between Steepest Descent and Newtons Method." *Neural Computation,* **4**, 141-166. https://doi.org/10.1162/neco.1992.4.2.141.

Bilim, C., Atiş, C. D., Tanyildizi, H., Karahan, O. (2009). Predicting the compressive strength of ground granulated blast furnace slag concrete using artificial neural network. Advances in Engineering Software, **40**(5), 334-340, https://doi.org/10.1016/j.advengsoft.2008.05.005.

Both, K., Fellinger, J. and Twilt, L. (1997), "Shallow floor construction with deep composite deck: from fire tests to simple calculation rules", Heron. 42(3), 145-158. http://heronjournal.nl/42-3/2.pdf.

Brownlee, J. (2016), "Master Machine Learning Algorithms: Discover How They Work and Implement Them From Scratch", Machine Learning Mastery.

BS 476-20 (1987) British Standards Institution, "BS 476-20 - fire tests on building materials and structures, in: Method for Determination of the Fire Resistance of Elements of Construction (General Principles), London.

EN1994-1-2 (2009) CEN European Committee for Standardization, EN 1994-1-2, Eurocode 4: Design of composite steel and concrete structures, BSI British Standards, Brussels.

Du, K.L. and Swamy, M.N. (2013). *Neural networks and statistical learning.* Springer Science & Business Media.

Duan, Z. H., Kou, S. C., Poon, C. S. (2013). Prediction of compressive strength of recycled aggregate concrete using artificial neural networks. Construction and Building Materials, 40, 1200-1206, https://doi.org/10.1016/j.conbuildmat.2012.04.063.

Duan, J., Asteris, P.G., Nguyen, H. et al. (2020). A novel artificial intelligence technique to predict compressive strength of recycled aggregate concrete using ICA-XGBoost model. Engineering with Computers (2020). https://doi.org/10.1007/s00366-020-01003-0.

Ellobody, E. (2011), "Nonlinear behaviour of unprotected composite slim floor steel beams exposed to different fire conditions", Thin-Wall. Struct., 49(6), 762-771. https://doi.org/10.1016/j.tws.2011.02.002.

Gupta, R., Gijzen van, M.B. and Vuik, C.K. (2013). "Efficient Two-Level Preconditioned Conjugate Gradient Method on the GPU." In *High Performance Computing for Computational Science - VECPAR 2012*, edited by O. Marques M. Daydé and K. Nakajima, 36–49. Springer, Berlin. https://doi.org/10.1007/978-3-642-38718-0_7.

Huang, L., Asteris, P.G., Koopialipoor, M., Armaghani, D.J., Tahir, M.M. (2019), "Invasive Weed Optimization Technique-Based ANN to the Prediction of Rock Tensile Strength", Appl. Sci. **9**, 5372, https://doi.org/10.3390/app9245372.

ISO 834 (1999), "834: Fire resistance tests-elements of building construction", Proceedings of the International Organization for Standardization, Geneva, Switzerland.

Kayacan, E. and Khanesar, M.A. (2015). *Fuzzy Neural Networks for Real Time Control Applications: Concepts, Modeling and Algorithms for Fast Learning.* 1. Butterworth-Heinemann.

Kechagias, J., Tsiolikas, A., Asteris, P., Vaxevanidis, N. (2018), "Optimizing ANN performance using DOE: Application on turning of a titanium alloy", MATEC Web of Conferences, 178, 01017, https://doi.org/10.1051/matecconf/201817801017

Kim, H.J., Kim, H.Y. and Park, S.Y. (2011), "An experimental study on fire resistance of Slim Floor beam", Appl. Mech. Mater., 82, 752-757. https://doi.org/10.4028/www.scientific.net/AMM.82.752.

Le, TT., Asteris, P.G. & Lemonis, M.E. (2021). Prediction of axial load capacity of rectangular concrete-filled steel tube columns using machine learning techniques. Engineering with Computers (2021). https://doi.org/10.1007/s00366-021-01461-0.

Lourakis, M.I.A. (2005), "A brief description of the Levenberg-Marquardt algorithm implemented by levmar", Hellas (FORTH), Institute of Computer Science Foundation for Research and Technology, http://www.ics.forth.gr/~lourakis/levmar/levmar.

Ly, H.B., Pham, B.T., Le, L.M., Le, T.T., Le, V.M., and Asteris, P.G. (2021), "Estimation of axial load-carrying capacity of concrete-filled steel tubes using surrogate models", *Neural Computing and Applications*, **33**(8), 3437-3458. https://doi.org/10.1007/s00521-020-05214-w

Ma, Z. and Mäkeläinen, P. (2000), "Behavior of composite slim floor structures in fire", J. Struct. Eng., 126(7), 830-837. https://doi.org/10.1061/(ASCE)0733-9445(2000)126:7(830).

Ma, Z. and Mäkeläinen, P. (2006), "Structural behaviour of composite slim floor frames in fire conditions", J. Constr. Steel Res., 62(12), 1282-1289, https://doi.org/10.1016/j.jcsr.2006.04.026.

Mäkeläinen, P. and Ma, Z. (2000), "Fire resistance of composite slim floor beams", J. Constr. Steel Res., 54(3), 345-363. https://doi.org/10.1016/S0143-974X(99)00059-0.

Maraveas, C., Wang, Y.C., Swailes, T., (2013) "Thermal and Mechanical properties of 19th century fireproof flooring systems at elevated temperatures", Constr. Build. Mat., 48, 248-264. https://doi.org/10.1016/j.conbuildmat.2013.06.084

Maraveas, C., Wang, Y.C., Swailes, T., (2014) "Fire resistance of 19th century fireproof flooring systems: a sensitivity analysis", Constr. Build. Mat., 55, 69-81. https://doi.org/10.1016/j.conbuildmat.2014.01.022

Maraveas, C. (2014). "Numerical analysis of DELTA composite beams in fire", Proceedings of the 7th European conference on steel and composite structures—EUROSTEEL.

Maraveas, C. (2017a), "Fire resistance of DELTABEAM® composite beams: a numerical investigation", J. Struct.Fire Eng., 8(4), 338-353. https://doi.org/10.1108/JSFE-05-2016-0003.

Maraveas, C., Wang, Y.C., Swailes, T., (2017a), "Reliability based determination of material safety factor for cast iron beams in jack arched construction exposed to standard and natural fires", Fire Saf. J., 90, 44-53, https://doi.org/10.1016/j.firesaf.2017.04.007

Maraveas, C., Fasoulakis, Z. and Tsavdaridis, K. (2017b), "Fire resistance of axially restrained and partially unprotected Ultra Shallow Floor Beams (USFB®) and DELTABEAM® composite beams", Proceedings of the Applications of Structural Fire Engineering. http://hdl.handle.net/2268/215370.

Maraveas, C., Tsavdaridis, K. and Nadjai, A. (2017c), "Fire resistance of unprotected ultra shallow floor beams (USFB): A numerical investigation", Fire Technol., 53(2), 609-627. https://doi.org/10.1007/s10694-016-0583-5.

Maraveas, C., Swailes, T. and Wang, Y. (2012), "A detailed methodology for the finite element analysis of asymmetric slim floor beams in fire", Steel Constr., 5(3), 191-198. https://doi.org/10.1002/stco.201210024.

Marquardt, D. (1963). "An Algorithm for Least-Squares Estimation of Nonlinear Parameters." *Journal of the Society for Industrial and Applied Mathematics,* **11**, 431-441. https://doi.org/10.1137/0111030.

Memarzadeh A, Shahmansouri A.A., Nematzadeh M., Gholampour A., (2021). "A review on fire resistance of steel concrete composite slim floor beams" *Steel and Composite Structures*, 40(1), 13-32, https://doi.org/10.12989/scs.2021.40.1.013

Møller, M.F. (1993). "A scaled conjugate gradient algorithm for fast supervised learning." *Neural Networks*, **6**, 525-533.

https://doi.org/10.1016/S0893-6080(05)80056-5.

Momeni, E., Armaghani, D.J., Hajihassani, M. and Amin, M.F.M. (2015), “Prediction of uniaxial compressive strength of rock samples using hybrid particle swarm optimization-based artificial neural networks”, *Measurement*, **60**, 50-63. https://doi.org/10.1016/j.measurement.2014.09.075.

Özcan, F., Atiş, C. D., Karahan, O., Uncuoğlu, E., Tanyildizi, H. (2009). Comparison of artificial neural network and fuzzy logic models for prediction of long-term compressive strength of silica fume concrete. Advances in Engineering Software, 40(9), 856-863, https://doi.org/10.1016/j.advengsoft.2009.01.005.

Powell, M.J.D. (1977). "Restart procedures for the conjugate gradient method." *Mathematical Programming*, **12**, 241-254. https://doi.org/10.1007/BF01593790.

Psyllaki, P., Stamatiou, K., Iliadis, I., Mourlas, A., Asteris, P., Vaxevanidis, N. (2018), "Surface treatment of tool steels against galling failure", MATEC Web of Conferences, 188, 04024, https://doi.org/10.1051/matecconf/201818804024.

Raghuwanshi, N.S., Singh, R. and Reddy, L.S. (2006). "Runoff and Sediment Yield Modeling Using Artificial Neural Networks: Upper Siwane River, India." *Journal of Hydrologic Engineering*, **11**, 71-79. https://doi.org/10.1061/(ASCE)1084-0699(2006)11:1(71).

Romero, M.L., Cajot, L.G., Conan, Y. and Braun, M. (2015), “Fire design methods for slim-floor structures″, Steel Construction. 8(2), 102-109, https://doi.org/10.1002/stco.201510012.

Romero, M.L., Albero, V., Espinós, A. and Hospitaler, A. (2019), “Fire design of slim-floor beams″, Stahlbau, 88(7), 665-674. https://doi.org/10.1002/stab.201900030.

Romero, M.L., Espinós, A., Lapuebla-Ferri, A., Albero, V. and Hospitaler, A. (2020), “Recent developments and fire design provisions for CFST columns and slim-floor beams”, J. Constr. Steel Res., 172, 106159.

Rumelhart, D.E., Hinton, G.E. and Williams, R.J. (1986). "Learning representations by back-propagating errors." *Nature*, **323**, 533-536. https://doi.org/10.1038/323533a0.

Sarir, P., Chen, J., Asteris, P.G., Armaghani, D.J. and Tahir, M.M. (2019). "Developing GEP tree-based, neuro-swarm, and whale optimization models for evaluation of bearing capacity of concrete-filled steel tube columns." *Engineering with Computers.* https://doi.org/10.1007/s00366-019-00808-y.

Taormina, R., Chau, K. and Sethi, R. (2012). "Artificial neural network simulation of hourly groundwater levels in a coastal aquifer system of the Venice lagoon." *Engineering Applications of Artificial Intelligence*, **25**, 1670-1676. https://doi.org/10.1016/j.engappai.2012.02.009.

Vos de, N.J. and Rientjes, T.H.M. (2008). "Multiobjective training of artificial neural networks for rainfall-runoff modeling." *Water Resources Research*, **44**. https://doi.org/10.1029/2007WR006734.

Walnman, D. E. (1996) “Technical Note – Preliminary assessment of the data arising from a standard fire test performed on a Slimflor beam at the Warrington Fire Research Centre on 14 Feb 1996, test No. WFRC 66162,” British Steel, UK.

Zaharia, R. and Franssen, J.M. (2012), “Simple equations for the calculation of the temperature within the cross-section of slim floor beams under ISO Fire”, Steel Compos.Struct., 13(2), 171-185, https://doi.org/10.12989/scs.2012.13.2.171.

Zeng, J.; Asteris, P.G.; Mamou, A.P.; Mohammed, A.S.; Golias, E.A.; Armaghani, D.J.; Faizi, K.; Hasanipanah, M. (2021), “The Effectiveness of Ensemble-Neural Network Techniques to Predict Peak Uplift Resistance of Buried Pipes in Reinforced Sand”, Appl. Sci. 2021, 11, 908. https://doi.org/10.3390/app11030908.

Zeng, J.; Roussis, P.C.; Mohammed, A.S.; Maraveas, C.; Fatemi, S.A.; Armaghani, D.J.; Asteris, P.G. (2021). Prediction of Peak Particle Velocity Caused by Blasting through the Combinations of Boosted-CHAID and SVM Models with Various Kernels. Appl. Sci. 2021, 11, 3705. https://doi.org/10.3390/app11083705

Zhang, H., Nguyen, H., Bui, XN. *et al*. (2021), “A generalized artificial intelligence model for estimating the friction angle of clays in evaluating slope stability using a deep neural network and Harris Hawks optimization algorithm”, Engineering with Computers (2021). https://doi.org/10.1007/s00366-020-01272-9.